Introduction to Lidar Remote Sensing (Ceilometer)

Ruben Delgado
Joint Center for Earth Systems Technology
University of Maryland, Baltimore County

Planetary Boundary Layer Workshop 2020
July 16, 2020

Ceilometer

- Device for measuring and recording the height of clouds
- Device for measuring the height of cloud bases and overall cloud thickness.
- Measures cloud base height and vertical visibility in all weather - good or bad.
- Measures cloud height and vertical visibility for meteorological and aviation applications.

Ceilometer

- Based on LIDAR (light detection and ranging) technology.
- Elastic Backscatter Lidar
- Instrument transmits fast, low-power laser pulses into the atmosphere and detects back-scattered returns from clouds and aerosols above the instrument.
- Advancement in technology in the last decade has made ceilometer/lidar affordable ($30,000).

Elastic Backscatter Lidar

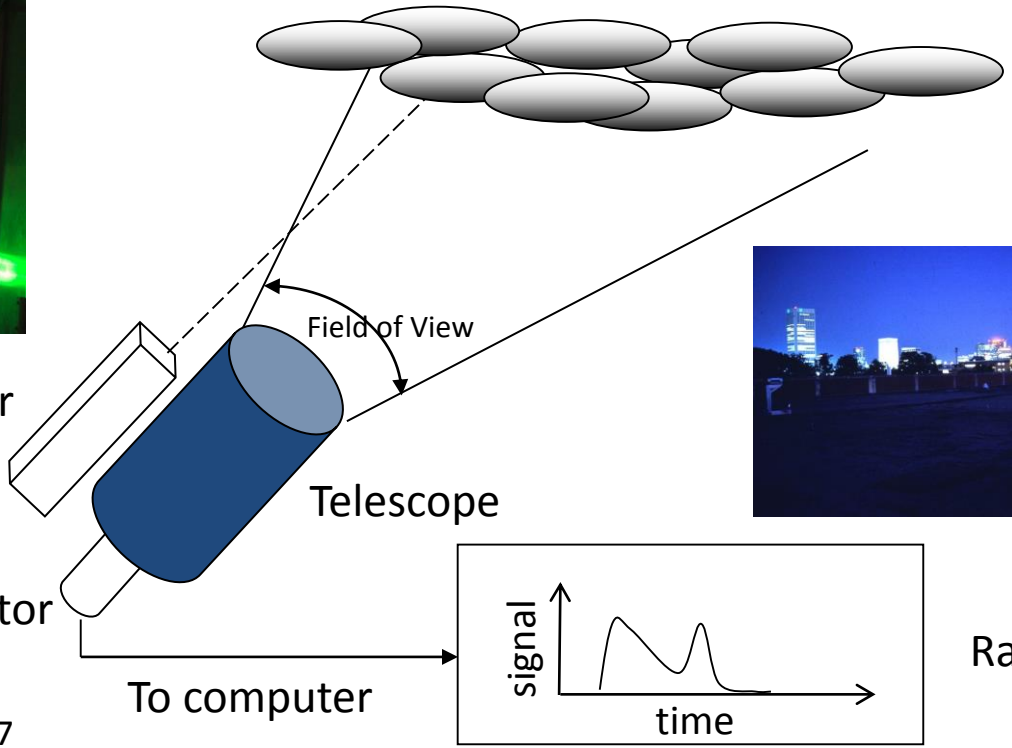

Adapted D. Roberts AMS 2007

Range Determination from TOF

- Modern atmosphere lidars: Due to the use of nanosecond pulse lasers, the range can be determined by the time-of-flight through equation $R = c \cdot \Delta t/2$, where c is the light speed in the medium, Δt is the time-of-flight, and 2 for the round-trip of the photons traveled.
- Because atmospheric scatters are distributed sources, i.e., scattered signals are continuous, the ultimate resolution of range determination is limited by the pulse duration time τ.
- Ultimate resolution: $\Delta R = c \cdot \tau/2$
- For example, a 5-ns pulse gives 75 cm as the highest resolution for an atmospheric lidar.

Overview of Physical Processes in Lidar

- Light propagation in the atmosphere or medium:
  - Light transmission vs. light extinction (attenuation)
  - Extinction (attenuation) = Absorption + Scattering (Total)
- Interaction between light and objects

(1) Scattering (instantaneous elastic & inelastic):
  - Mie, Rayleigh, and Raman scattering

(2) Absorption and differential absorption

(3) Laser induced fluorescence

(4) Resonance fluorescence

(5) Doppler shift and Doppler broadening

(6) Boltzmann distribution

(7) Reflection from target or surface

Scattering

Scattering fundamentals

- Scattering can be broadly defined as the *redirection of radiation out of the original direction of propagation*, usually due to interactions with molecules and particles
- Reflection, refraction, diffraction etc. are actually all just forms of scattering
- Matter is composed of discrete electrical charges (atoms and molecules – dipoles)
- Light is an oscillating EM field – excites charges, which radiate EM waves
- These radiated EM waves are *scattered waves*, excited by a source external to the scatterer
- The *superposition of incident and scattered EM waves* is what is observed

Scattering geometry

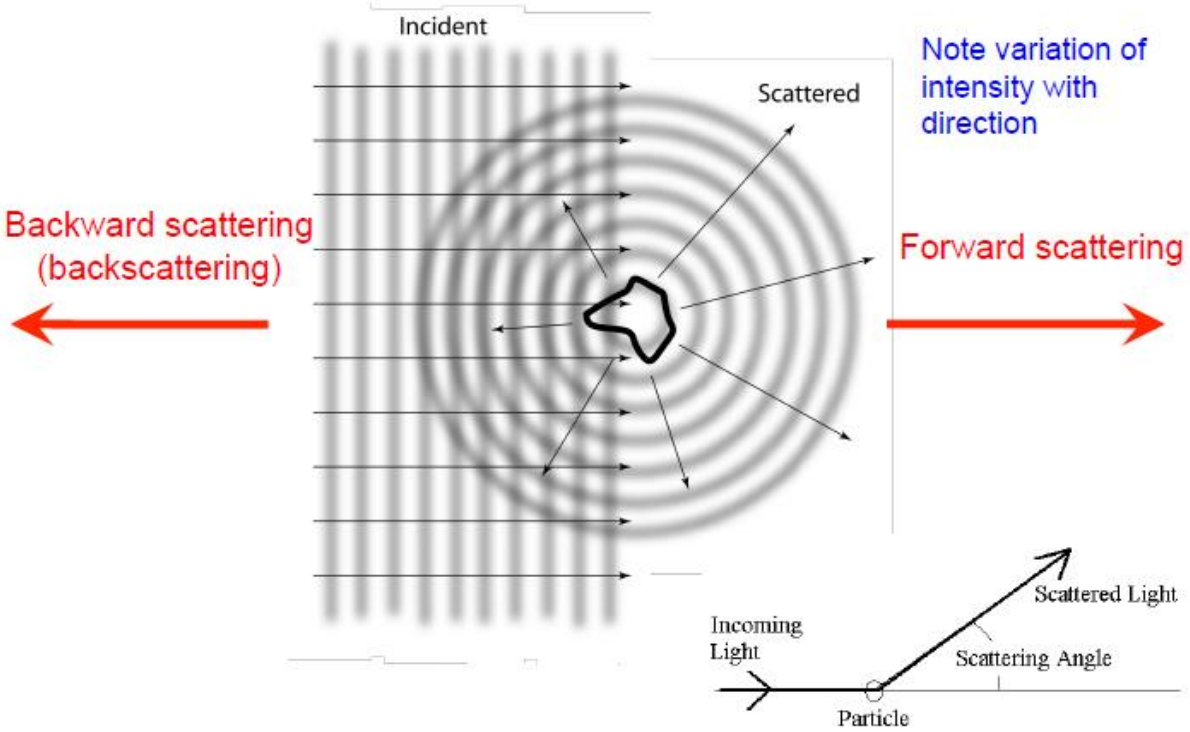

Types of scattering

- Elastic scattering – the wavelength (frequency) of the scattered light is the same as the incident light (*Rayleigh and Mie scattering*)

- Inelastic scattering – the emitted radiation has a wavelength different from that of the incident radiation (*Raman scattering, fluorescence*)

- Quasi-elastic scattering – the wavelength (frequency) of the scattered light shifts (e.g., in moving matter due to Doppler effects)

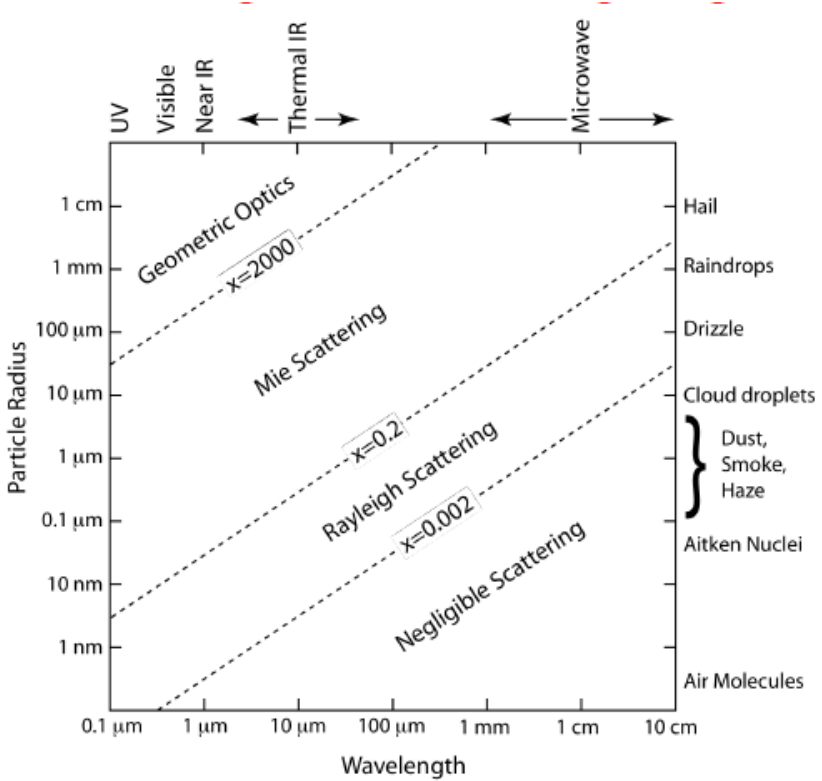

Elastic Scattering

- Wavelength does not change upon scattering
- Rayleigh scattering is for particles small compared to λ
  - Varies as λ^{-4}
- Mie scattering applies *only* to spherical particles comparable to λ
  - Varies as $\sim\lambda^{-2}$ to $\sim\lambda^{+1}$
- Mie scattering parameter α defined as $\alpha = 2\pi r/\lambda$
  - r is the characteristic dimension of the scattering particle

- H.C. van de Hulst "Light Scattering by Small Particles," Dover Publications
- C.F. Bohren and D.R. Huffman, "Absorption and Scattering of Light by Small Particles," Wiley Science Paperback Series

Extinction of radiation

- $\beta_e = \beta_a + \beta_s$

- The extinction coefficient (β_e) is the sum of an absorption coefficient (β_a) and a scattering coefficient (β_s) – all have units of inverse length (m^{-1})
- For milk, $\beta_a \approx 0$ so $\beta_e \approx \beta_s$; for ink $\beta_s \approx 0$ so $\beta_e \approx \beta_a$
- To characterize the relative importance of scattering and absorption in a medium, the single scatter albedo (ω) is used:

$$\omega = \frac{\beta_s}{\beta_e} = \frac{\beta_s}{\beta_s + \beta_a}$$

- $\omega = 0$ for a purely absorbing medium (ink), 1 in a purely scattering medium (milk)

Elastic Backscatter Lidar

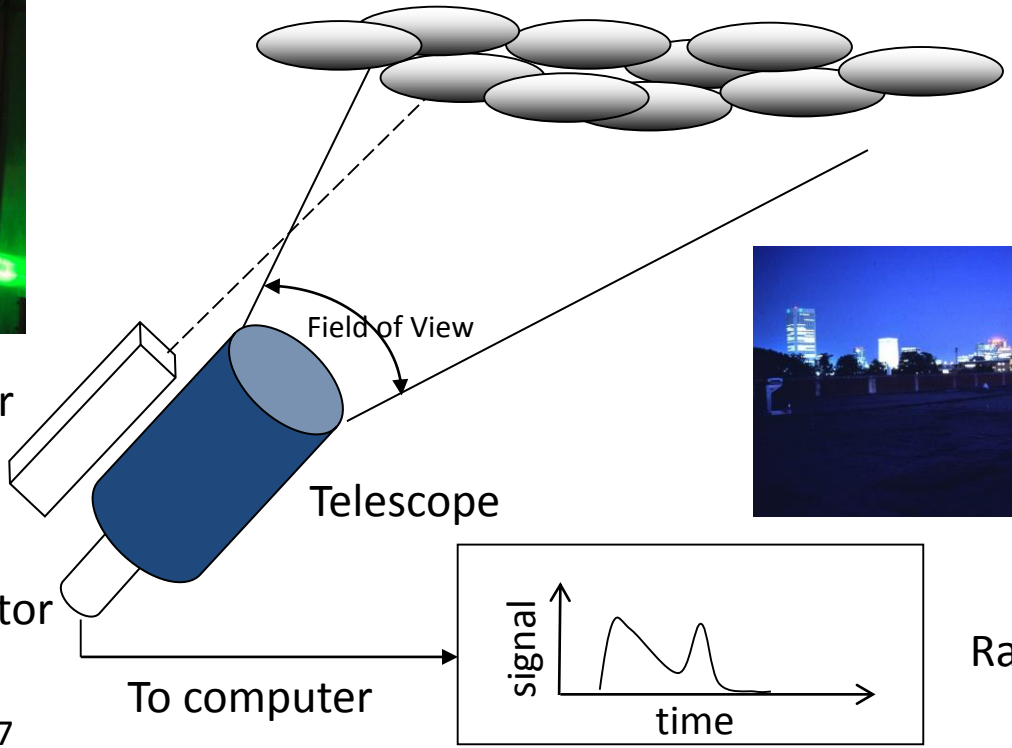

Adapted D. Roberts AMS 2007

Lidar Transmitter/Receiver Configurations

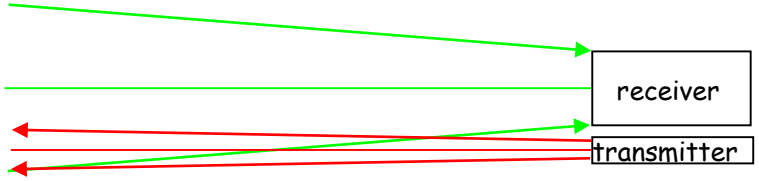

- Bistatic
  - Transmitter and receiver have parallel optic axes separated by a short distance

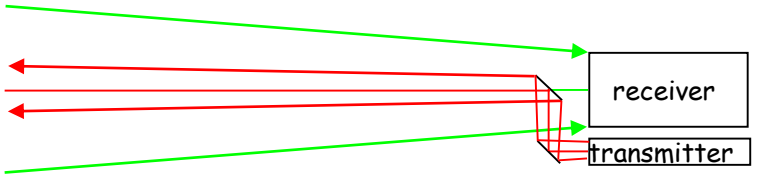

- Coaxial
  - Transmitter beam emerges from the center of the receiver aperture

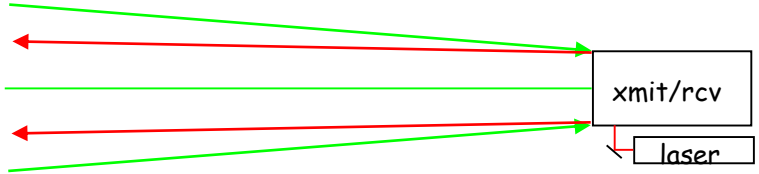

- Common Optics
  - Transmitter and receiver use the same optics

Adapted D. Roberts AMS 2007

Lidar Transmitter Components

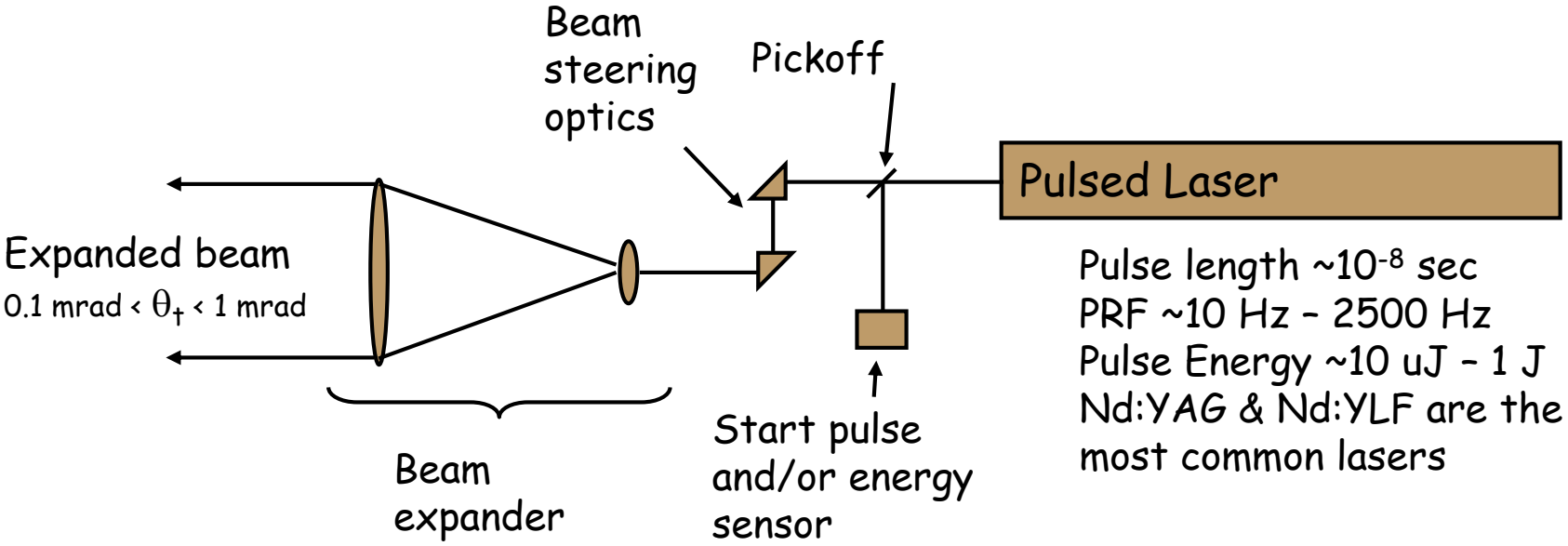

Adapted D. Roberts AMS 2007

Lidar Receiver Components

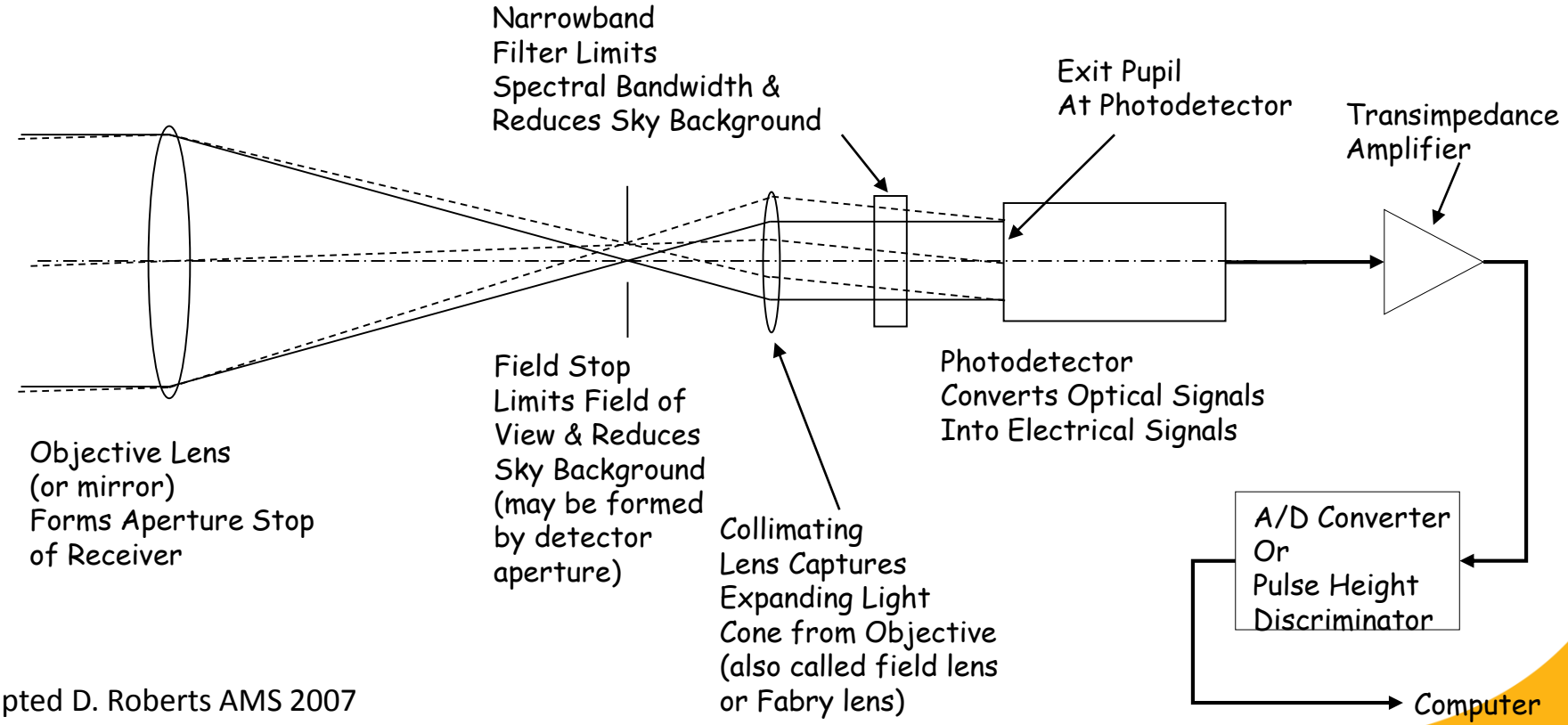

Adapted D. Roberts AMS 2007

Lidar Equation

$$N_S(\lambda,R) = N_L(\lambda_L)\cdot \eta(\lambda_L)\cdot T(\lambda_L,R)\cdot \left[\beta(\lambda,\lambda_L,\theta,R)\Delta R\right]\cdot T(\lambda,R)\cdot \frac{A}{R^2}\cdot \eta(\lambda)\cdot G(R) + N_B$$

- In general, the interaction between the light photons and the particles is a scattering process.
- The expected photon counts are proportional to the product of the

(1) transmitted laser photon number,

(2) probability that a transmitted photon is scattered,

(3) probability that a scattered photon is collected,

(4) light transmission through medium, and

(5) overall system efficiency.

- Background photon counts and detector noise also contribute to the expected photon counts.

Factors of Lidar Equation

The received photon counts N_S are related to the factors

$$N_S(\lambda,R) \propto$$

$$N_L(\lambda_L)$$ Transmitted laser photon number

$$T(\lambda_L,R)$$ Laser photon transmission through medium

$$\beta(\lambda,\lambda_L,\theta,R)\cdot\Delta R$$ Probability of a transmitted photon to be scattered

$$T(\lambda,R)$$ Signal photon transmission through medium

$$\frac{A}{R^2}$$ Probability of a scattered photon to be collected

$$\eta(\lambda,\lambda_L)G(R)$$ Lidar system efficiency and geometry factor

Basic Assumptions of Lidar Equation

- The lidar equation is developed under two assumptions: the scattering processes are independent, and only single scattering occurs.

- Independent scattering means that particles are separated adequately and undergo random motion so that the contribution to the total scattered energy by many particles have no phase relation. Thus, the total intensity is simply a sum of the intensity scattered from each particle.

- Single scattering implies that a photon is scattered only once. Multiple scatter is excluded in our considerations.

1st Term: Transmitted Photon Number

$$N_S(\lambda,R) = N_L(\lambda_L)\cdot\left[\beta(\lambda,\lambda_L,\theta,R)\Delta R\right]\cdot\frac{A}{R^2}\cdot\left[T(\lambda_L,R)T(\lambda,R)\right]\cdot\left[\eta(\lambda,\lambda_L)G(R)\right]+N_B$$

$$N_L(\lambda_L) = \left(\frac{P_L(\lambda_L)\Delta t}{hc/\lambda_L}\right)$$

$$= \frac{\text{Laser Power x time bin length}}{\text{Planck constant x Laser frequency}}$$

$$= \frac{\text{Transmitted laser energy within time bin}}{\text{Single laser photon energy}}$$

$$= \text{Transmitted laser photon number within time bin length}$$

2nd Term: Probability to be Scattered

$$N_S(\lambda,R) = N_L(\lambda_L)\cdot\left[\beta(\lambda,\lambda_L,\theta,R)\Delta R\right]\cdot\frac{A}{R^2}\cdot\left[T(\lambda_L,R)T(\lambda,R)\right]\cdot\left[\eta(\lambda,\lambda_L)G(R)\right]+N_B$$

Angular scattering probability – the probability that a transmitted photon is scattered by scatters into a unit solid angle.

Angular scattering probability =
volume scatter coefficient β
x scattering layer thickness ΔR

Volume Scatter Coefficient β

Volume scatter coefficient β is equal to

$$\beta(\lambda,\lambda_L,R)=\sum_i\left[\frac{d\sigma_i(\lambda_L,\theta)}{d\Omega}n_i(R)\,p_i(\lambda)\right] \quad (m^{-1}sr^{-1})$$

$\frac{d\sigma_i(\lambda_L)}{d\Omega}$ is the differential scatter cross-section of single particle in species i at scattering angle θ (m^2sr^{-1})

$n_i(R)$ is the number density of scatter species i (m^{-3})

$p_i(\lambda)$ is the probability of the scattered photons falling into the wavelength λ.

Volume scatter coefficient β is the probability per unit distance travel that a photon is scattered into wavelength λ in unit solid angle at angle θ.

3rd Term: Probability to be Collected

$$N_S(\lambda,R) = N_L(\lambda_L)\cdot\left[\beta(\lambda,\lambda_L,\theta,R)\Delta R\right]\cdot\frac{A}{R^2}\cdot\left[T(\lambda_L,R)T(\lambda,R)\right]\cdot\left[\eta(\lambda,\lambda_L)G(R)\right]+N_B$$

The probability that a scatter photon is collected by the receiving telescope, i.e., the solid angle subtended by the receiver aperture to the scatterer.

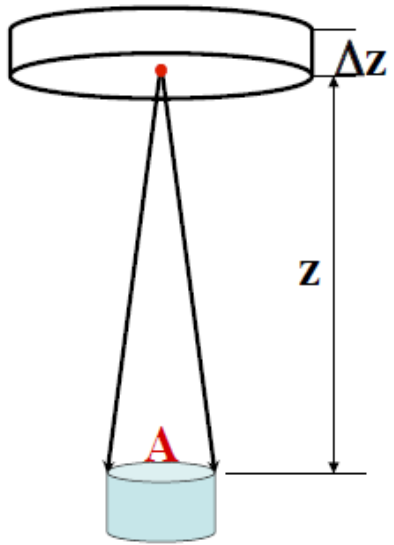

4th Term: Light Transmission

$$N_S(\lambda,R) = N_L(\lambda_L)\cdot\left[\beta(\lambda,\lambda_L,\theta,R)\Delta R\right]\cdot\frac{A}{R^2}\cdot\left[T(\lambda_L,R)T(\lambda,R)\right]\cdot\left[\eta(\lambda,\lambda_L)G(R)\right]+N_B$$

The atmospheric transmission of laser light at outgoing wavelength λ_L and return signal at wavelength λ

Transmission for laser light →

$$T(\lambda_L,R) = \exp\left[-\int_0^R \alpha(\lambda_L,r)dr\right]$$

Transmission for return signal →

$$T(\lambda,R) = \exp\left[-\int_0^R \alpha(\lambda,r)dr\right]$$

Where $\alpha(\lambda_L, R)$ and $\alpha(\lambda, R)$ are extinction coefficients (m^{-1})

Extinction Coefficient α

$$\alpha(\lambda,R) = \sum_i \left[\sigma_{i,ext}(\lambda) n_i(R)\right]$$

$\sigma_{i,ext}(\lambda)$ is the extinction cross-section of species i

$n_i(R)$ is the number density of species i

Extinction = Absorption + Scattering (Integrated)

$$\sigma_{i,ext}(\lambda) = \sigma_{i,abs}(\lambda) + \sigma_{i,sca}(\lambda)$$

Total Extinction = Aerosol Extinction + Molecule Extinction

$$\alpha(\lambda,R) = \alpha_{aer,abs}(\lambda,R) + \alpha_{aer,sca}(\lambda,R) + \alpha_{mol,abs}(\lambda,R) + \alpha_{mol,sca}(\lambda,R)$$

5th Term: Overall Efficiency

$$N_S(\lambda,R) = N_L(\lambda_L)\cdot\left[\beta(\lambda,\lambda_L,\theta,R)\Delta R\right]\cdot\frac{A}{R^2}\cdot\left[T(\lambda_L,R)T(\lambda,R)\right]\cdot\left[\eta(\lambda,\lambda_L)G(R)\right]+N_B$$

$\eta(\lambda,\lambda_L) = \eta_T(\lambda_L)\cdot\eta_R(\lambda)$ is the lidar hardware optical efficiency

e.g., mirrors, lens, filters, detectors, etc

$G(R)$ is the geometrical form factor, mainly concerning the overlap of the area of laser irradiation with the field of view of the receiver optics

6th Term: Background Noise

$$N_S(\lambda,R) = N_L(\lambda_L)\cdot\left[\beta(\lambda,\lambda_L,\theta,R)\Delta R\right]\cdot\frac{A}{R^2}\cdot\left[T(\lambda_L,R)T(\lambda,R)\right]\cdot\left[\eta(\lambda,\lambda_L)G(R)\right]+N_B$$

N_B is the expected photon counts due to background noise, detector and circuit shot noise, etc.

Up-looking lidar: main background noise comes from solar scattering, solar straight radiation, star/city light.

Down-looking lidar: besides above noise, it could have three extra backgrounds: (1) Specular reflection from water/ice surface; (2) Laser reflectance from ground; (3) Solar reflectance from ground.

$$N_S(\lambda,R) = N_L(\lambda_L)\cdot \eta(\lambda_L)\cdot T(\lambda_L,R)\cdot \left[\beta(\lambda,\lambda_L,\theta,R)\Delta R\right]\cdot T(\lambda,R)\cdot \frac{A}{R^2}\cdot \eta(\lambda)\cdot G(R) + N_B$$

- N_S -- expected photon counts detected at λ and R
- 1st term -- the transmitted laser photon number;
- 2nd term -- the probability of a transmitted photon to be scattered by the objects into a unit solid angle;
- 3rd term -- the probability of a scatter photon to be collected by the receiving telescope;
- 4th term -- the light transmission through medium for the transmitted laser and return signal photons;
- 5th term -- the overall system efficiency;
- 6th term N_B -- background and detector noise counts.

Physical Picture of Lidar Equation

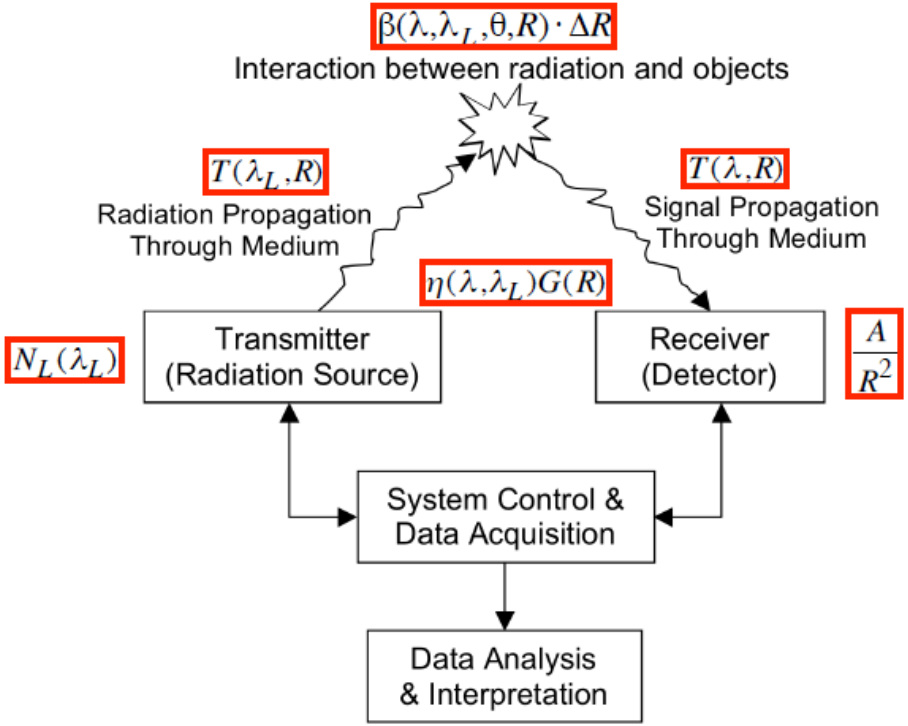

Illustration of Lidar Equation

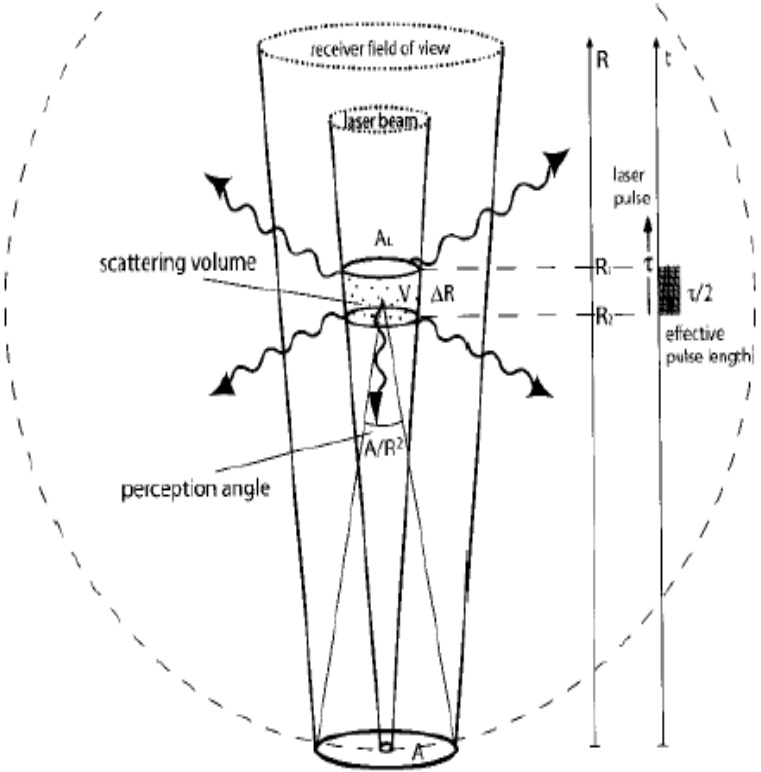

What can elastic backscatter lidar do?

- Reveal atmospheric structure
  - Aerosol layer distribution
  - Cloud location and structure
  - Boundary layer growth and dynamics
  - Plume monitoring
- Single-ended measurement of
  - extinction and/or backscatter coefficient versus range
  - partial optical depth to a given altitude
  - transmission along a path

Measuring Our Changing World

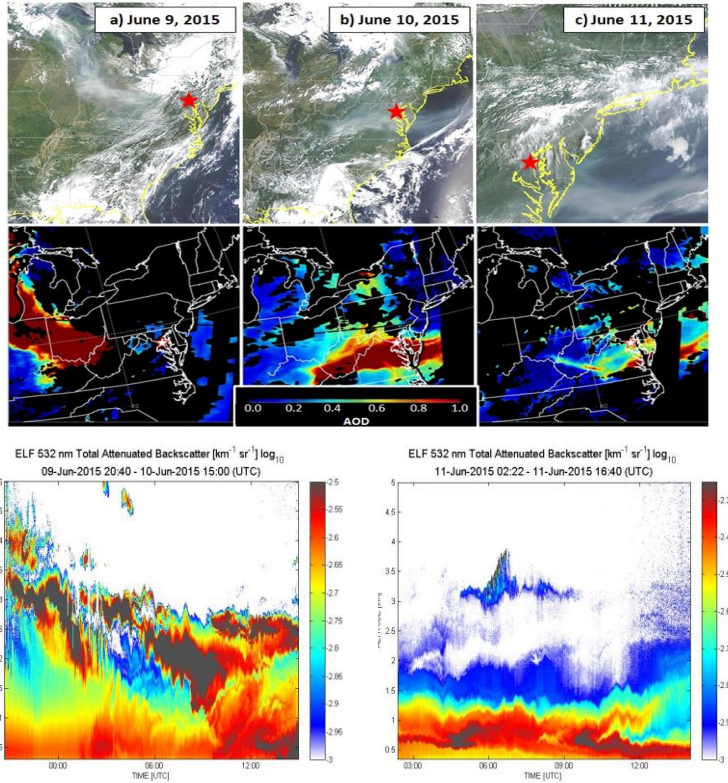

Dressen et al., "Observations and impacts of transported Canadian wildfire smoke on ozone and aerosol air quality in the Maryland region on June 9–12, 2015", JAWMA, 2016

Ceilometer/Lidar Remote Sensing

- Observational platform for pursuing societal benefits.
- Engagement between the scientific community and wide range of stakeholders.
- Provide information for managing land, water, air quality, agriculture, energy, disaster response and ecosystems functions.
  - Field Campaigns: DISCOVER-AQ, OWLETS, LISTOS

Planetary Boundary Layer (PBL) Monitoring

- Understanding the evolution of the **PBL** is crucial for air pollution as PBL dynamics control pollutant accumulation and dispersion, which in turn also influence aerosol-radiation PBL interactions
- Current observations are rarely available in the spatiotemporal scales needed to further our understanding of complex PBL dynamics. Ceilometers offer a low cost and reliable option for continuous measurements of the PBL.
- Ceilometers (Aerosol Backscatter) can monitor:
  - **Clouds and precipitation**
  - **PBL stratification**: residual layers, nocturnal boundary layers (NBL), lofted aerosol layers, etc.
  - **Synoptic changes influencing PBL dynamics**
  - **Impact of local circulation (bay/sea/lake/land breeze)**
  - **Strong shallow inversions**

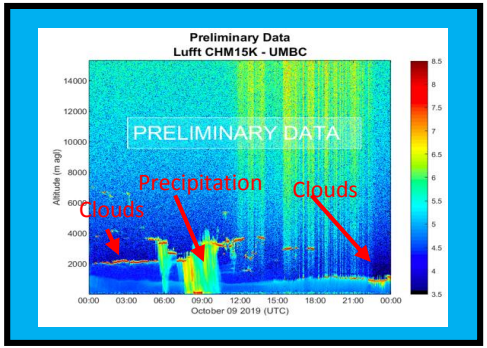

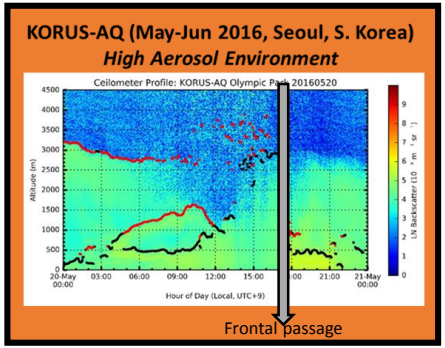

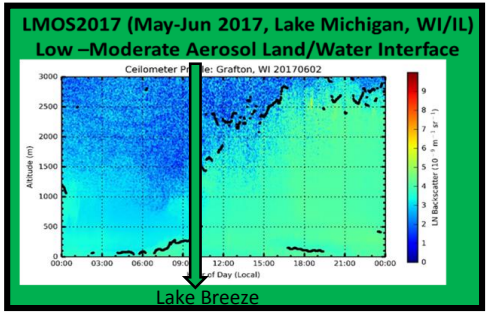

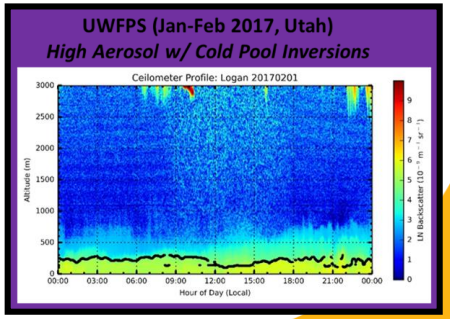

Observations Lead The Way

NRC

R. Hoff

Observing Weather and Climate from the Ground Up: A Nationwide Network of Networks (2009)

NSF

B. Demoz

Thermodynamic Profiling Technology Workshop (2011)

NASEM

R. Delgado

The Future of Atmospheric Boundary Layer Observing, Understanding, and Modeling (2018)

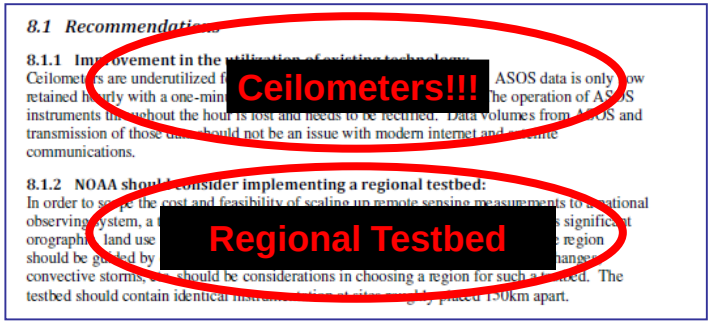

8.1 Recommendations

8.1.1 Improvement in the utilization of existing technology:
Ceilometers are underutilized f… ASOS data is only now retained hourly with a one-min… The operation of ASOS instruments throughout the hour is lost and needs to be rectified. Data volumes from ASOS and transmission of those data should not be an issue with modern internet and satellite communications.

Ceilometers!!!

8.1.2 NOAA should consider implementing a regional testbed:
In order to scope the cost and feasibility of scaling up remote sensing measurements to a national observing system, a t… significant orographic land use … region should be guided by … change… convective storms … should be considerations in choosing a region for such a testbed. The testbed should contain identical instrumentation strategically placed 150km apart.

Regional Testbed

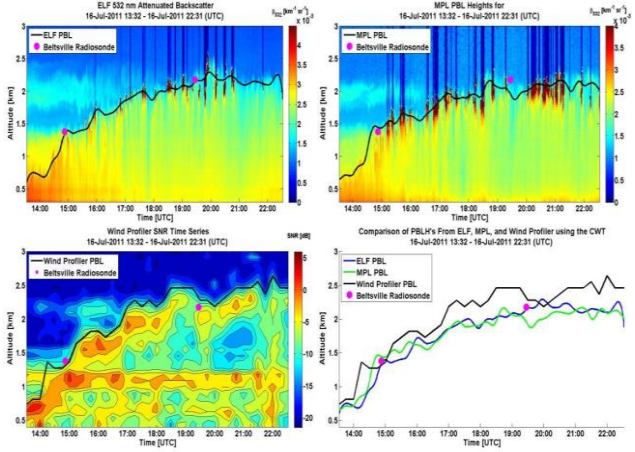

*Compton et al. (2013), J. Atmos. Ocean. Tech., doi:10.1175/JTECHD-12-00116.1

Boundary Layer Dynamics

PECAN: *3 June 2015 Bore Case*

Pictures taken at FP2

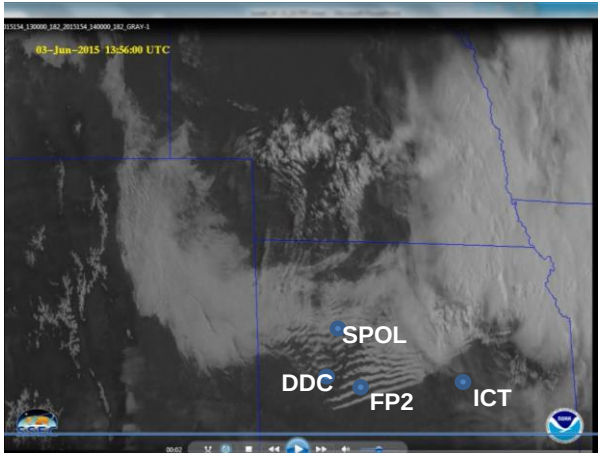

- Undular Bores are one of the suspected event that transport moisture upward priming the nighttime atmosphere for destabilization and severe storms.
- An accurate statistics of occurrence and observation is lacking, hence PECAN. This is bore case observed early on 3 June 2015, during PECAN.
- The CL31 network reveals the spatial evolution and duration of this bore.

PECAN: *3 June 2015 Bore Case*

CL31 network data from PECAN – no operational instrument is capable of capturing this event in such detail. Equivalent ASOS data is plotted, showing data lost

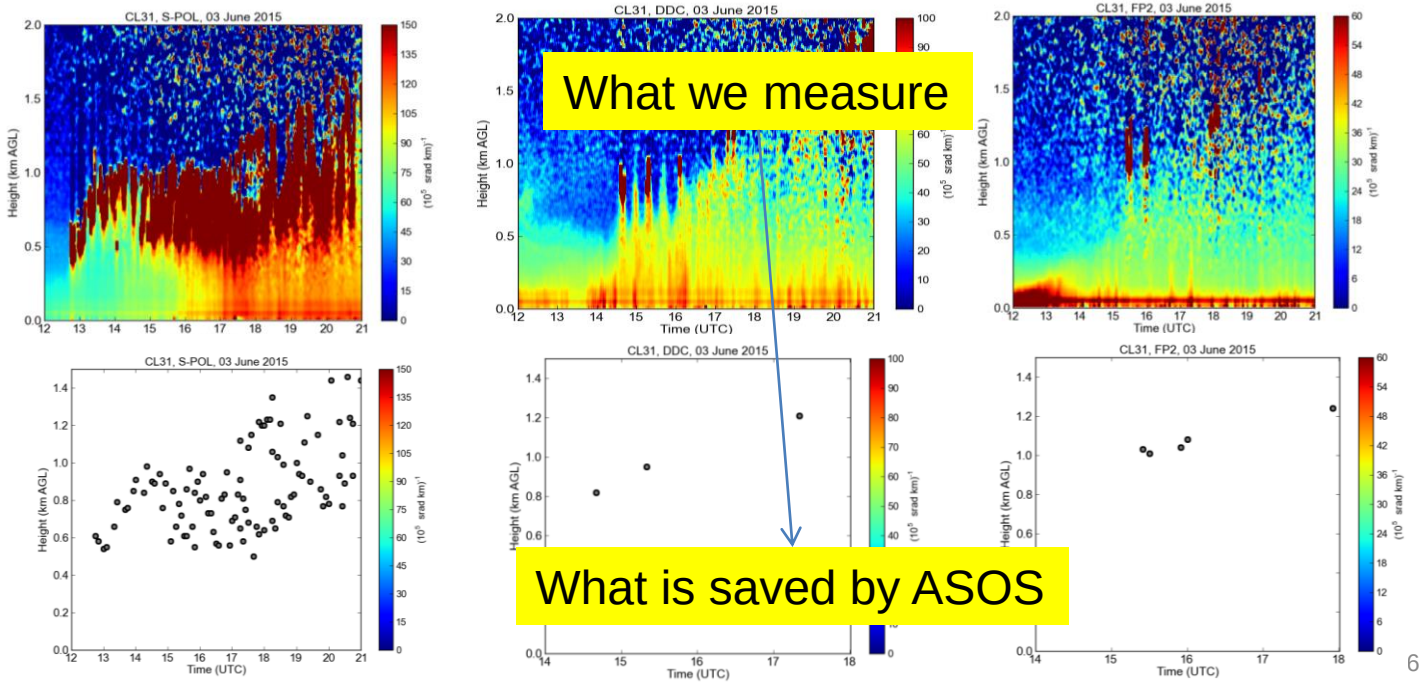

Ad-hoc Ceilometer Evaluation Study

- Joint Effort:
  - MDE/EPA/UMBC
  - Federal: NASA/NOAA
  - Academia: CCNY/Hampton and Howard University

- Measurements to help guide EPA PAMS program implementation for new hourly MLH requirement.

- Evaluation of Aerosol Backscatter and mixing layer height retrievals from commercial ceilometer/lidars (**software**):
  - **Campbell Scientific** CS135 and SkyVue Pro (**Viewpoint**)
  - **Leosphere** Windcube 200S (Windforge)
  - **Lufft:** CHM8k and CHM15k (**Lufft Viewer**)
  - **Vaisala:** CL31 and CL51 (**CL-View And BL-View**)

- Development of Common Algorithm for MLH

UMBC

Table 1. Commercial Ceilometer and software used			
Ceilometer	Logging Software	Resolution / Range / Reported Range	Reported Backscatter Corrections
Vaisala CL31	CL-View	10m / 0 – 7.7 km / 0 - 7.7 km	Background, range and overlap corrected
Vaisala CL51	BL-View	10m / 0 – 15 km / 0 – 4.5 km	Background, range and overlap corrected
Lufft CHM15k	Lufft Viewer	15m / 0 - 15 km / 0 – 15 km	Background, range and overlap corrected
Campbell Sci. CS135	Viewpoint	5m / 0 – 10 km / 0 – 10 km	Background, range and overlap corrected

Ceilometer Signal Evaluation


- Varying signal quality
  - QC/QA protocols per make/model
- Ceilometer signal evaluation/correction*
  - **Signal-to noise ratios**
  - **Overlap corrections**
  - **Artifacts**
  - Resolution

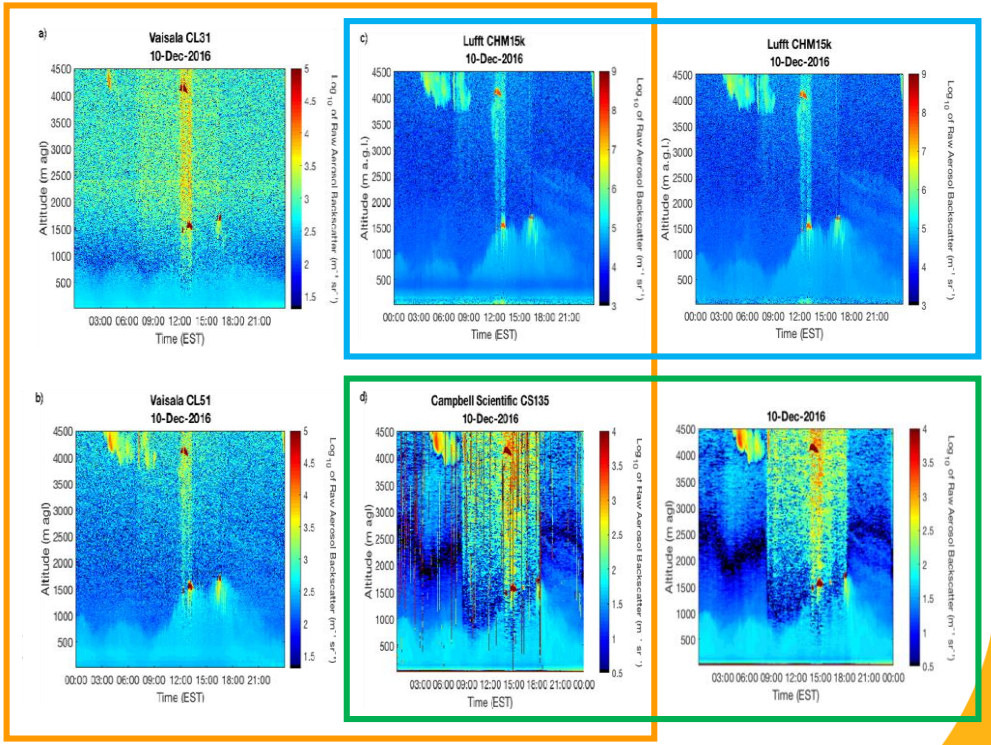

*(O'Connor et al., 2004; Wiegner and Geiss 2012; Hervo et al. 2016; Kotthaus et al. 2016, among others)

Commercial Software Evaluation

Software Evaluations: Lufft Interface Options

Web-based interface

- Requires static IP
  - Possibility at PAMS sites?
- Consistently falls out-of-sync with time
- Built in ftp transfer only with 1,5,10,15 minute options
- Internal SD card data storage

PC software

- Requires additional hardware
- Lufft PC software available for CHM15k only
- Allows for https transfers
- Internal SD card and PC data storage

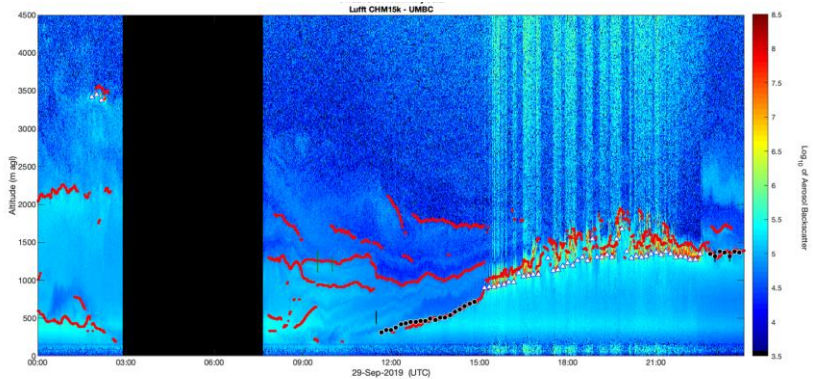

Commercial Software Evaluation

Software Evaluations: Vaisala BL-View 2.1.x

- CL-View (.dat) and BL-View (.his) files supported → no offline reprocessing/viewing
- Undescribed resolution (temporal and vertical) changes between L1, L2, L3 files in both .nc and .his formats
- Documentation insufficient:
  - Archive data imports
  - Variables in new .nc files are not described (quality index, extinction profiles, etc.)
- Licensing verification failure (licensing server unreachable) stops BL-View software
  - Data loss unless manually restarted
  - Serial splitter prevented data loss
  - Raspberry Pi data logging alternative is possible

Retrievals

- Hourly MLHs comparison to CWT retrievals
  - Treatment of cloud signals (cloud base/top interchangeable in retrievals)
  - ML growth delay
  - Determination of PBL during precipitation?

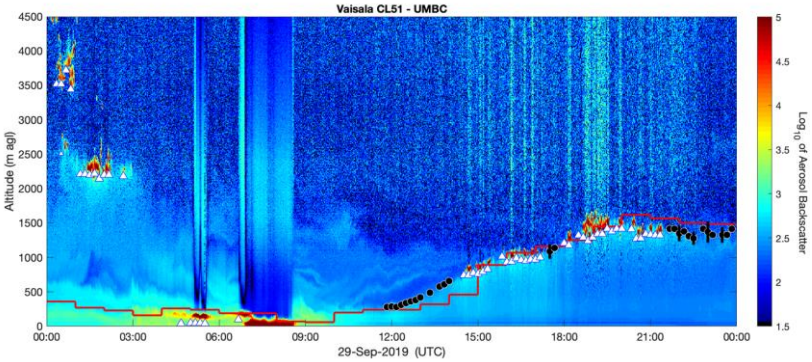

Commercial Software Evaluation

Lufft PBL heights

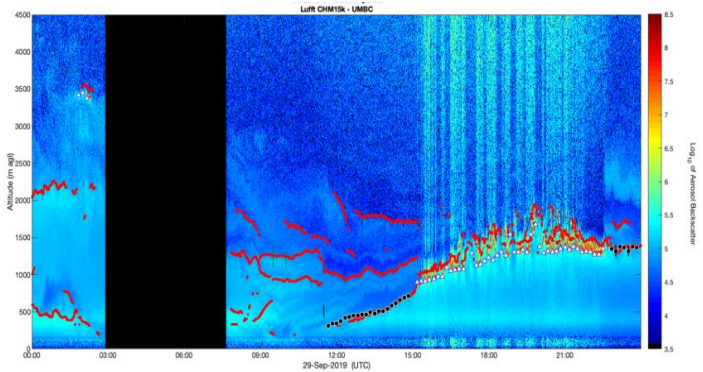

Software Evaluated

- Vaisala CL 51: BL-View
- Vaisala CL 31 : CL-View
- Campbell Scientific CS135: Viewpoint
- Lufft CHM8k and CHM15k: Lufft Viewer

Vaisala Hourly PBL heights

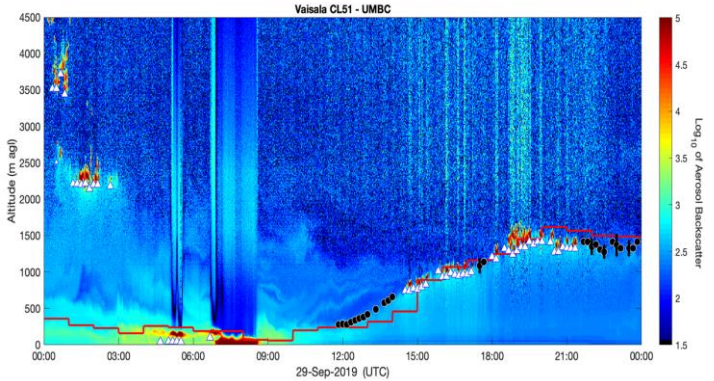

Campbell Sci. Cloud heights

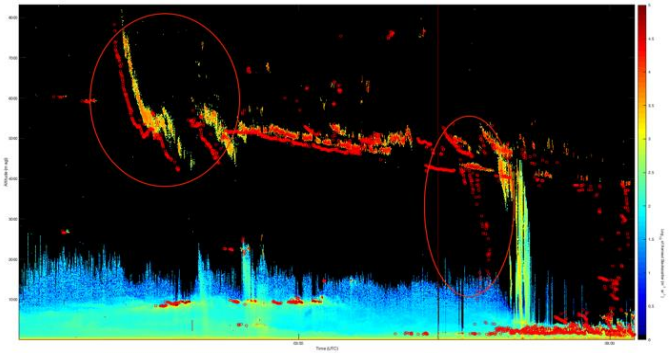

- CWT Set of rules
- CWT Clouds
- Commercial software

Planetary Boundary Layer Height Algorithm

Development of standardized retrieval algorithms for heterogeneous network

Covariance Wavelet Transform Algorithm

- **Automated** algorithm **corrects for instrument signal** quality and **automatically screens for precipitation and cloud layers**
- **Layer attribution** for the planetary boundary layer height with continuation and time-tracking parameters and uncertainty calculations through automatic filtering

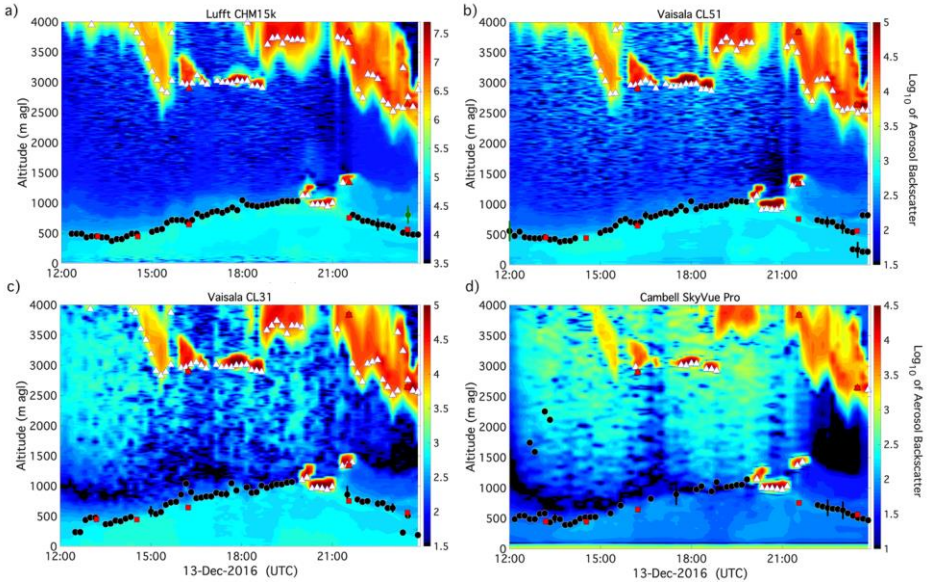

December 13, 2016 ($\overline{CWTC}$) profiles from CHM15k (a), CL51 (b), CL31(c), and SkyVue Pro (d) ceilometers. PBLH retrievals from the automated algorithm are displayed in black circles, while CBH retrievals are displayed as white triangles. Radiosonde heights for both PBLHs and CBH are displayed as red squares. Error bars display 10-minute retrieval uncertainties every 30 mins for display clarity purposes although uncertainties are calculated with every retrieval.

Caicedo et al. (2020) under review

"An automated common algorithm for planetary boundary layer retrievals using aerosol lidars in support of the U.S. EPA Photochemical Assessment Monitoring Sites Program"

Covariance Wavelet Transform

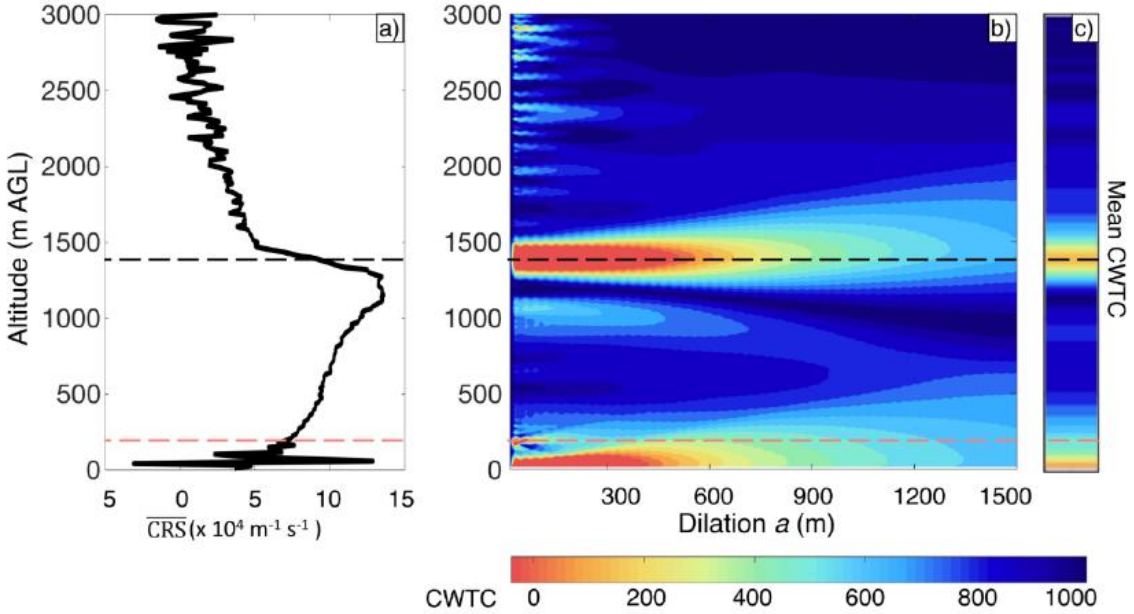

Haar Function

$$\psi_H\left(\frac{z-b}{a}\right) = \begin{cases} -1, & \text{if} \quad b - \frac{a}{2} \leqslant z \leqslant b \\ 1, & \text{if} \quad b \leqslant z \leqslant b + \frac{a}{2} \\ 0, & \text{elsewhere} \end{cases}$$

Covariance Wavelet

$$W_f(a,b) = \frac{1}{a}\int_{-\infty}^{\infty} f(z)\psi_H\left(\frac{z-b}{a}\right)dz$$

ψ_H = vertical distance or altitude
a = spatial extent or dilation of the function
b = center of the Haar function
$f(z)$ = Profile as a function of height (Corrected Return Signal (CRS))

Sharp gradients in the profile that are of interest are identified by local minima = PBLH

Caicedo et al. (2020) under review

Covariance Wavelet Transform

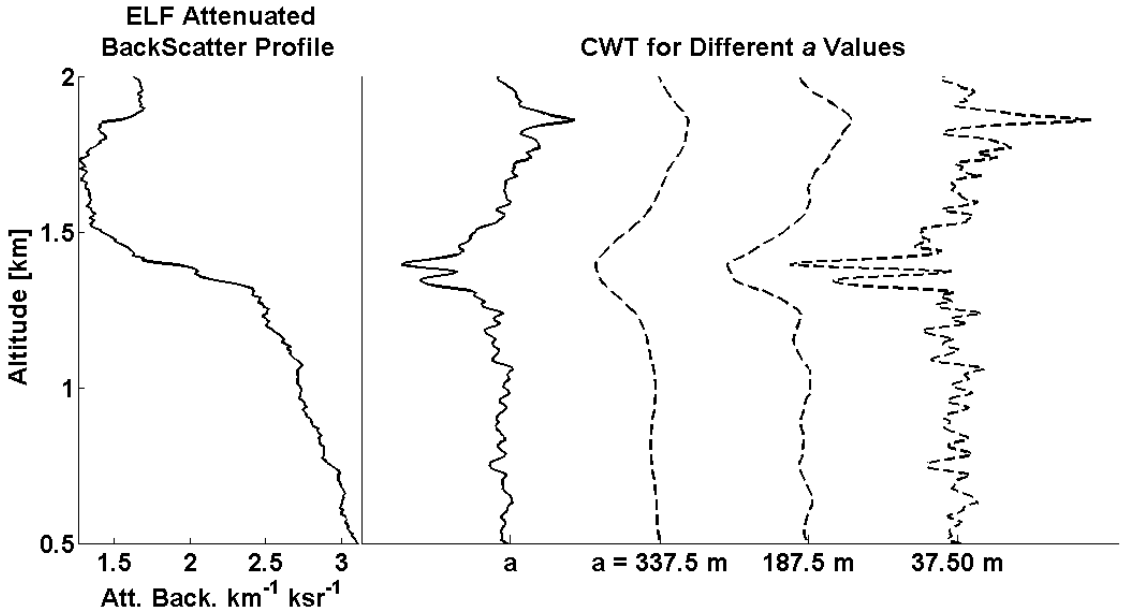

Compton et al., J. Atmos. Oceanic Technol. (2013)

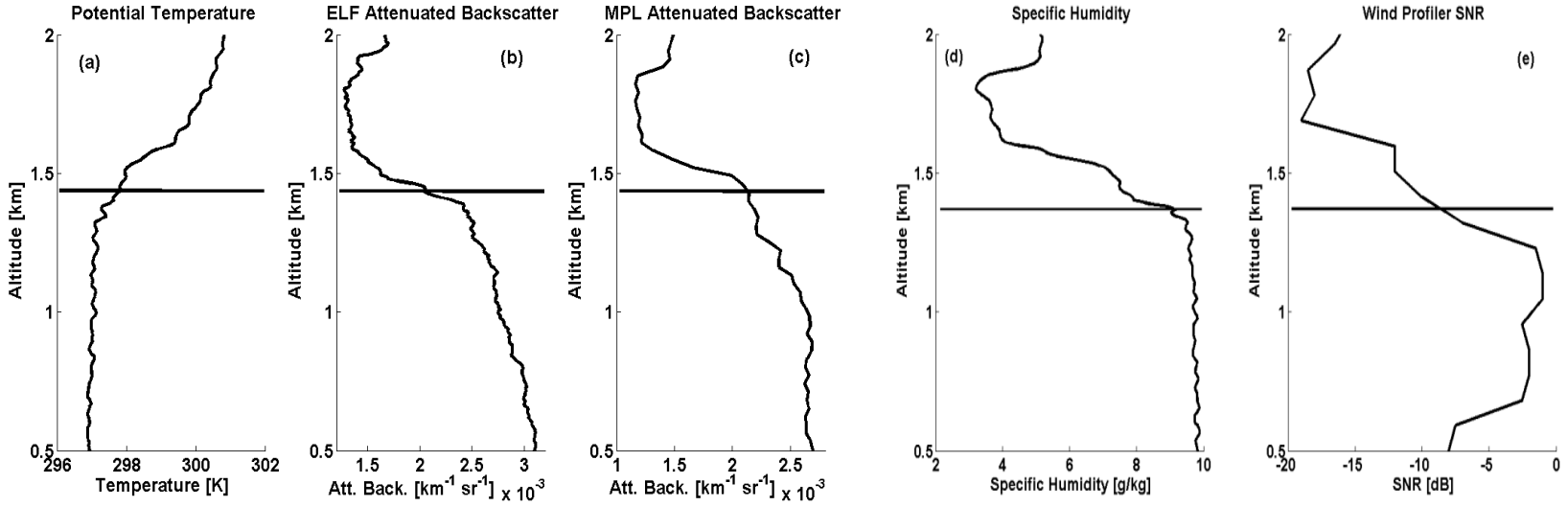

- The PBL is capped by a temperature inversion that occurs at the EZ that traps aerosols and moisture below.
- Above the temperature inversion, there are generally fewer aerosols and drier air.
- Radiosondes are used to measure the height of the potential temperature capping inversion.
- Vertical lidar backscatter and wind profiler SNR gradient is related to this temperature inversion

Compton et al., J. Atmos. Oceanic Technol. (2013)

PBL Evolution (Adapted from Stull)

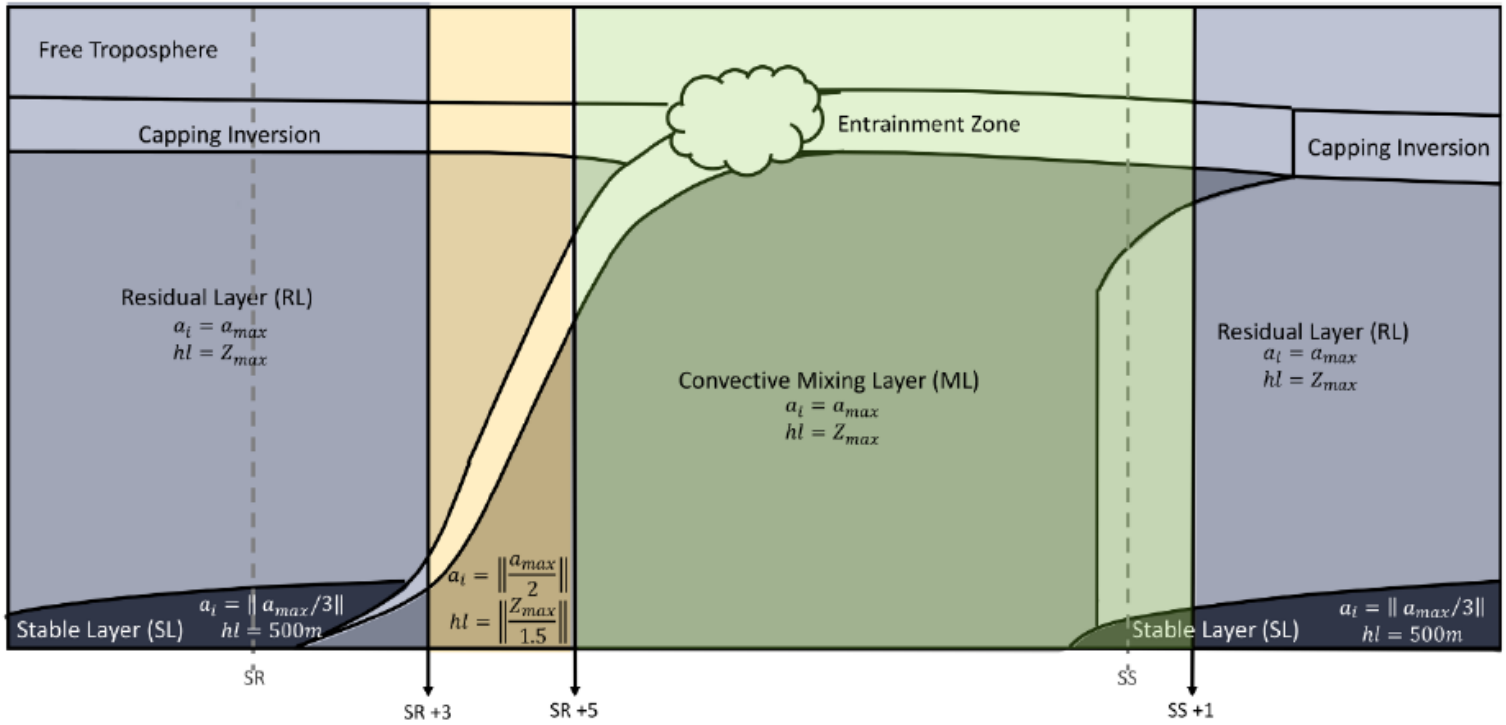

Evaluating PBL algorithms and methodologies

Algorithms were implemented to 10-minute averaged (preprocessed) aerosol backscatter

- Overall, low correlations seen across all ceilometers

		CHM15k	CS135	CL31	CL51
Haar wavelet	Slope	0.78	0.41	0.61	0.63
	Intercept	302.98	945.05	542.55	517.50
	r^2	0.74	0.13	0.40	0.50
	RMSE	243.92	509.67	401.03	334.29
Cluster analysis	Slope	0.42	0.23	0.13	0.28
	Intercept	616.03	713.34	1241.07	899.65
	r^2	0.23	0.17	0.02	0.12
	RMSE	410.05	249.02	461.05	387.20
Second Derivative	Slope	-0.06	0.03	0.02	0.12
	Intercept	1823.98	2144.73	1720.63	1741.24
	r^2	0.00	0.00	0.00	0.01
	RMSE	616.62	681.16	573.83	518.64

- Lowest correlations seen in CS135 due to instrument noise and artifacts
- Second derivative showed no correlation to radiosonde MLHs

Limitations: PBL algorithms

- Cloud signals create a strong negative gradient at the cloud layer top
- Without further characterization of cloud layers, an automated algorithm cannot correctly identify a MLH

		CHM15k	CS135	CL31	CL51
Haar wavelet	Slope	0.82	0.32	0.83	0.87
	Intercept	264.78	1045.89	238.60	233.69
	r^2	0.90	0.07	0.68	0.87
	RMSE	154.43	507.82	294.23	171.85
Cluster analysis	Slope	0.58	0.11	0.09	0.36
	Intercept	375.54	796.66	1278.44	762.73
	r^2	0.73	0.14	0.02	0.38
	RMSE	199.06	120.60	381.99	231.40
Second Derivative	Slope	-0.22	-0.13	-0.01	-0.07
	Intercept	2228.28	2602.76	1990.25	2174.34
	r^2	0.10	0.03	0.00	0.02
	RMSE	360.98	361.54	260.81	243.06

Cloud signals can account for up to 50% of entire data sets
(Caicedo et al., *2019*; Pearson et al., 2009; Lewis et al., 2013)

Limitations: PBL algorithms

- Multiple aerosol layers (lofted aerosol layers, residual layers, nocturnal surface layers, etc.)
- Implementation of continuity parameters and dual nighttime retrievals

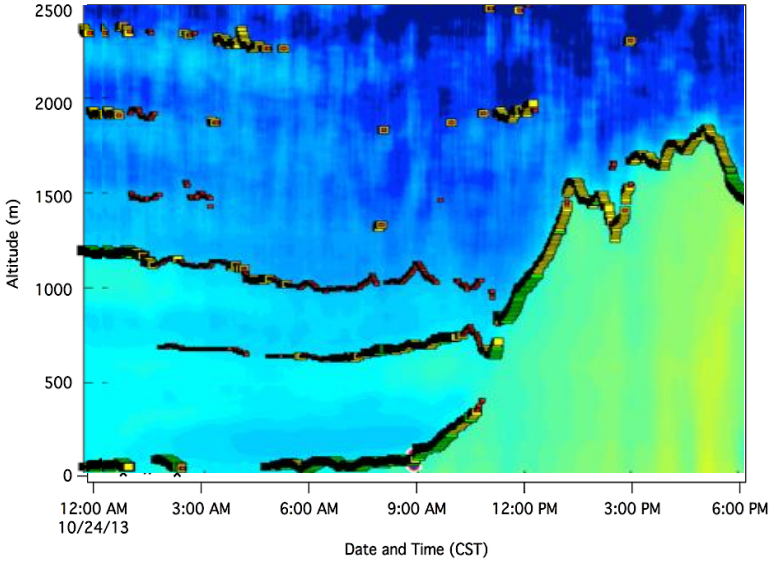

March 8, 2020 Controlled Burn Quantico, VA

- Location: U.S. Marine Corps Base in Quantico, VA
  - Near borders of Prince William, Stafford, and Fauquier Counties
- Controlled burn of ~2,000 acres
- Managed by Forestry Service of U.S. Marine Corps Quantico
  - U.S. Forest Service was not involved
- No advance warning of burn to local or state authorities
  - No state burn permits required
  - VA DEQ did not know (not part of air quality forecast)
  - There was an announcement on the Marine Corps Base Quantico's website about a controlled burn March 5 being postponed to March 6, but nothing about a burn on March 8
- Facebook posts (after the fact) about event from Quantico Fire and Emergency Services have since been deleted
  - Burn conducted 10 am to 1 pm
  - "We have been conducting back burns to control wildfires set by troop training in this area since Wednesday," officials said
  - Fire had to be started via helicopter, which contributed to the large smoke plume
  - "The burn out is complete and contained and smoke will disperse" (post late Sunday afternoon)

Weather Conditions (NAM)

- It was a terrible day to conduct a controlled burn
- Warm, very dry, light breeze:
  - High temp 63 °F (average 47 °F)
  - Dew point dropped from 25 °F at 12 UTC to 6 °F at 18 UTC (RH ~ 12%) as dry air mixed to surface
  - Winds S/SW at 7-12 mph, gusts 15-20 mph
- Strong surface inversion trapped smoke near surface
  - 12 UTC sounding shows surface inversion up to ~950 mb with secondary inversion aloft at ~875 mb
  - Surface inversion broke but inversion aloft remained; ceilometer data indicate mixing to ~ 1.1-1.2 km in afternoon
  - 00 UTC sounding shows persistent inversion aloft at ~925 mb

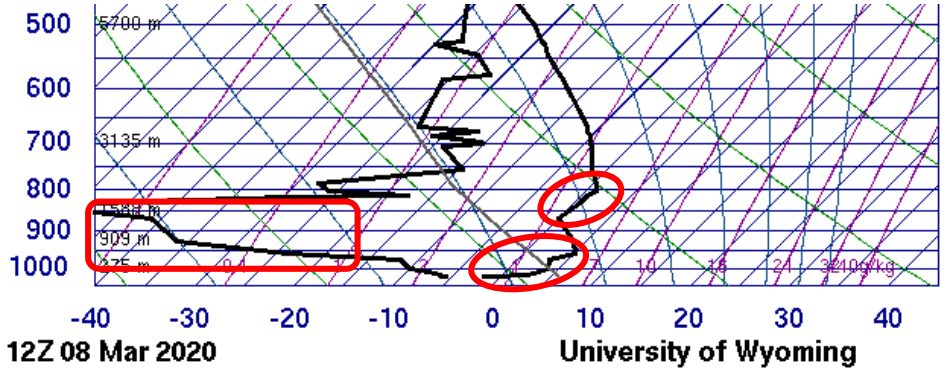

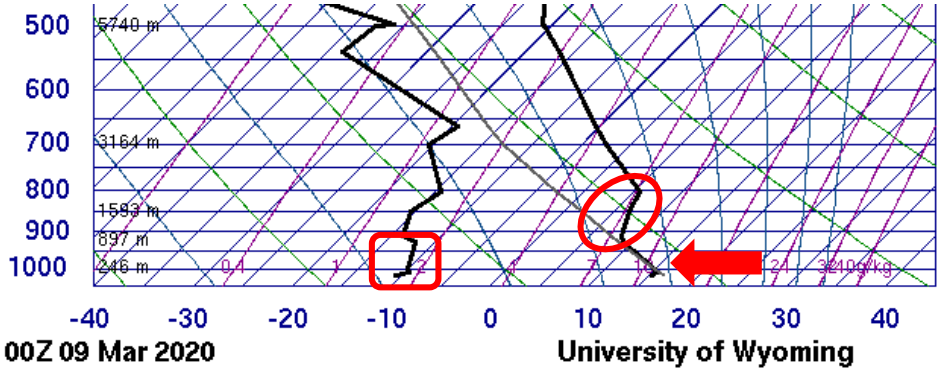

$PM_{2.5}$ Concentration from Transported Smoke

- Official monitors from AirNow network picked up transport of smoke moving northeast through DC, MD suburbs, Baltimore
  - Washington, DC @ 18:00-19:00 UTC
  - Near I-95/I-495 @ 20:00-21:00 UTC
  - Rockville/Laurel, MD @ 21:00-22:00 UTC
  - Downtown Baltimore @22:00-23:00 UTC
  - Northern metro Balt @ 23:00-00:00 UTC
- Many reports of haze, people smelling smoke

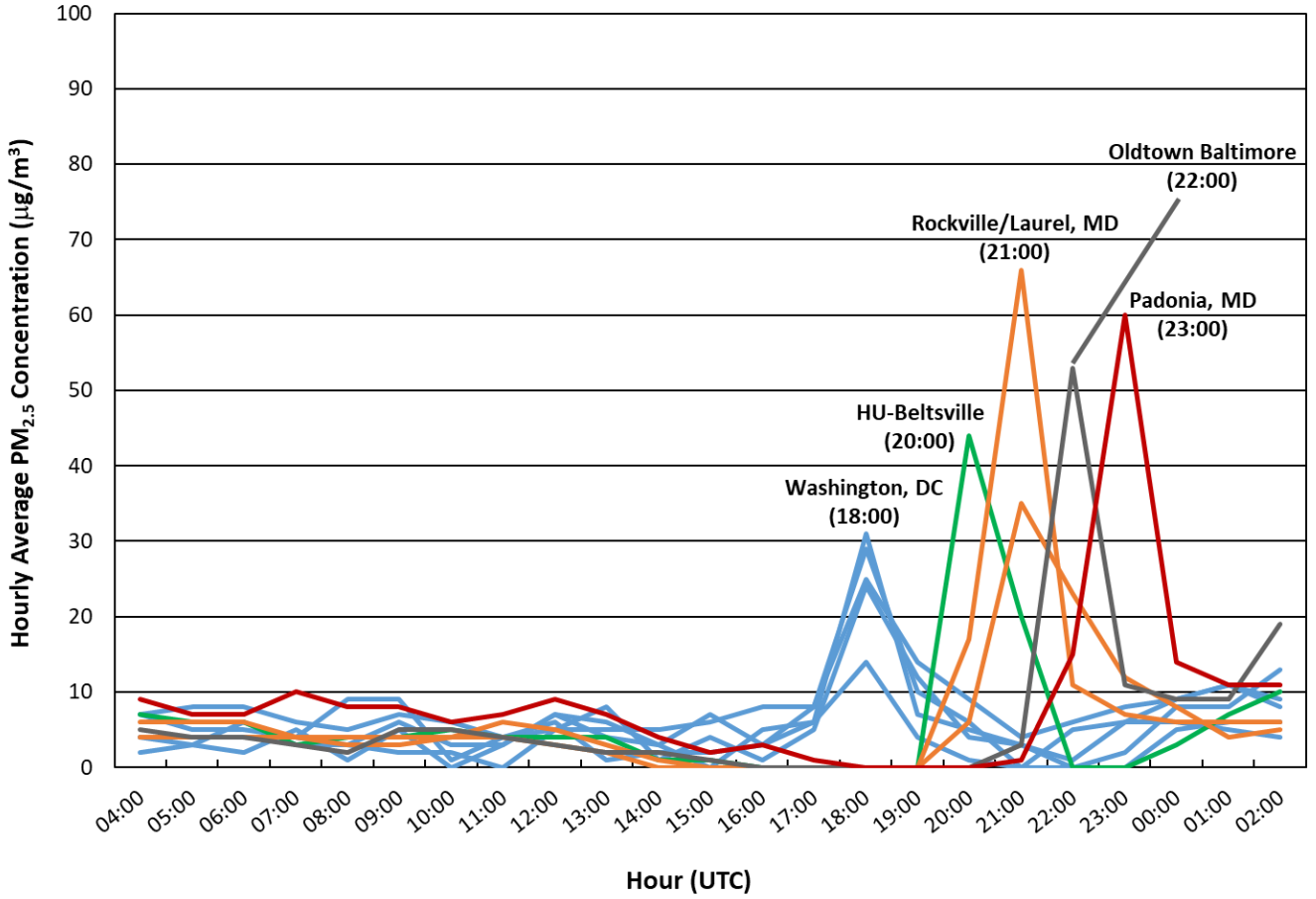

BC Concentration from Transported Smoke

- Increases in black carbon concentration (UV instrument) coincident with spikes in $PM_{2.5}$ concentration:
  - Near I-95/I-495 @ 20:00-22:00 UTC
  - Laurel, MD @ 21:00-22:00 UTC

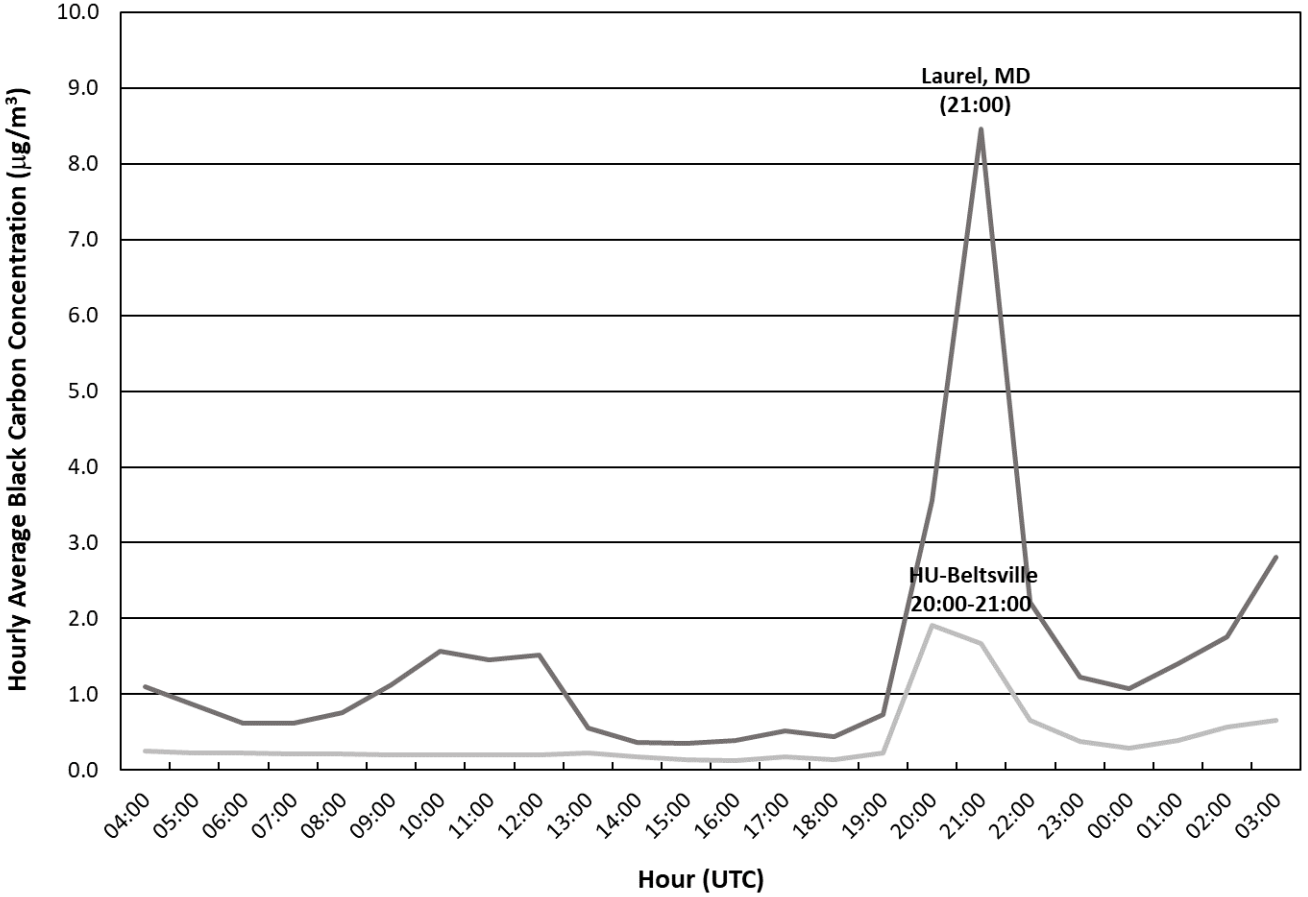

Ceilometer Data

- Preliminary data from ceilometer network shows similar story for timing of smoke transport
  - Washington, DC @ 19:00-20:00 UTC
  - Near I-95/I-495 @ 21:00-22:00 UTC
  - UMBC @ 22:00 UTC
  - Eastern metro Balt @ 23:00-00:00 UTC
- Also appears to be smoke aloft (previous days' burns?)

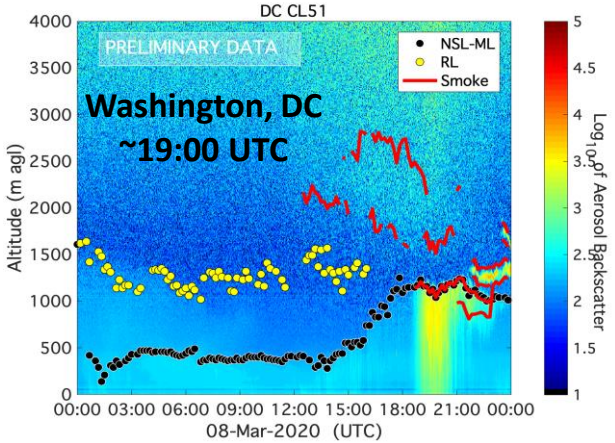

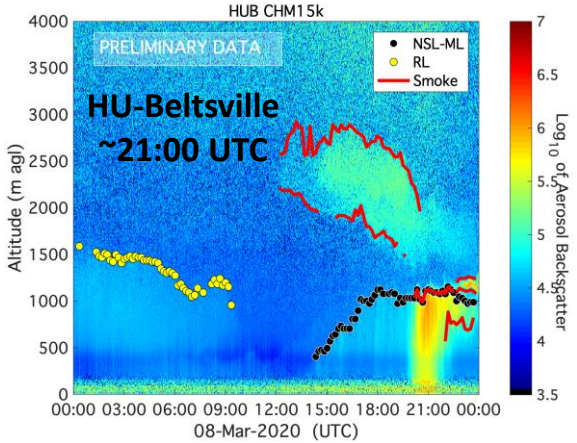

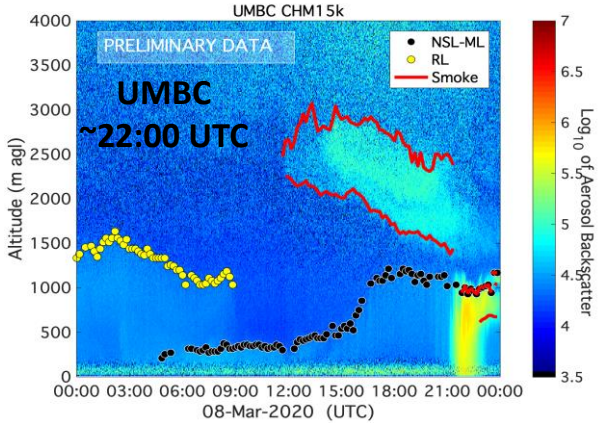

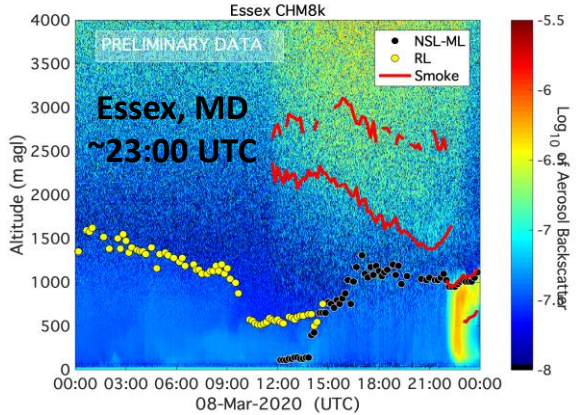

GOES-16 ABI AOD Captures Smoke Transport

- 15:00 UTC: MCBQ fire detected
- 15:30 UTC: smoke plume visible in ABI RGB
- 17:50 UTC: AOD picks up smoke plume (partial)
- 19:00 UTC: AOD picks up most of plume extent (DC metro area)
- 19:15 UTC: last MCBQ fire detection
- 20:00 UTC: AOD picks up plume from fire in western VA
- 21:00 UTC: AOD shows MCBQ plume move into MD suburbs
- 22:00 UTC: AOD shows MCBQ plume reaches Baltimore
- 22:15 UTC: last AOD imagery (sun sets at 23:10 UTC at KIAD)

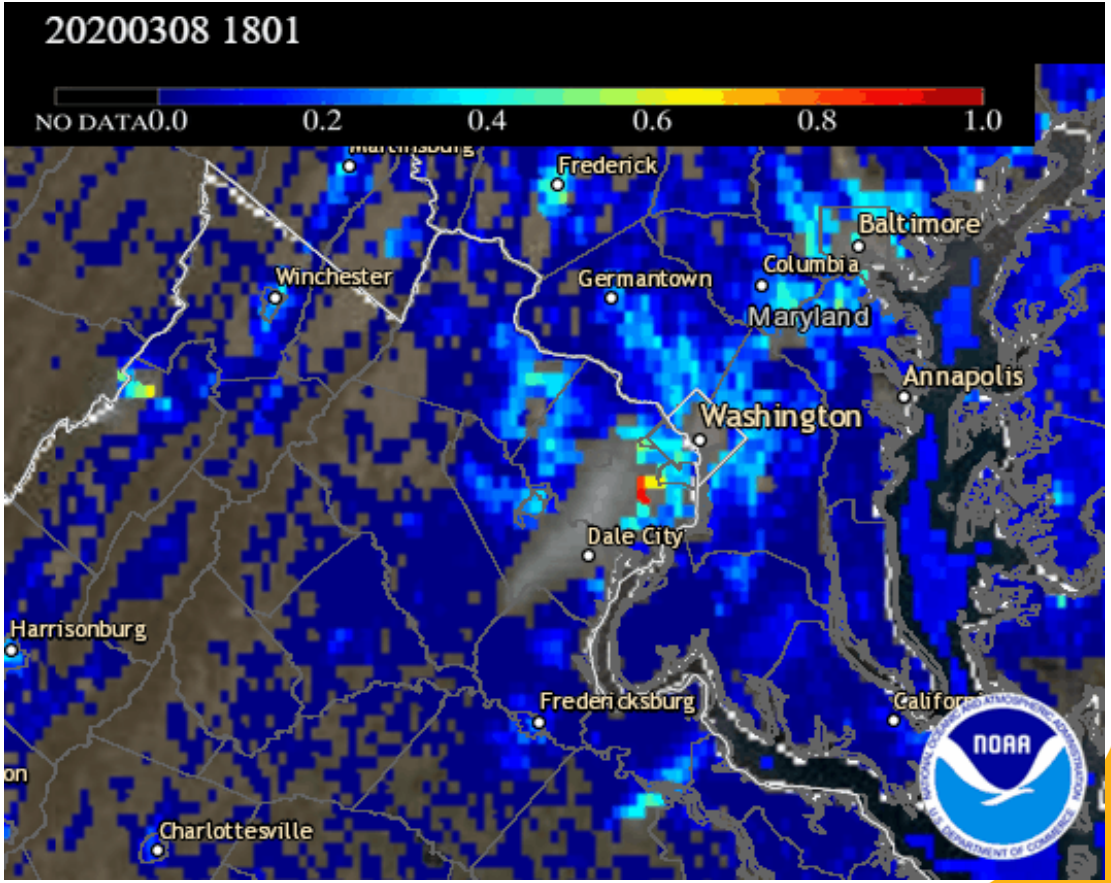

EPA AQ Profiler and Ceilometer Network

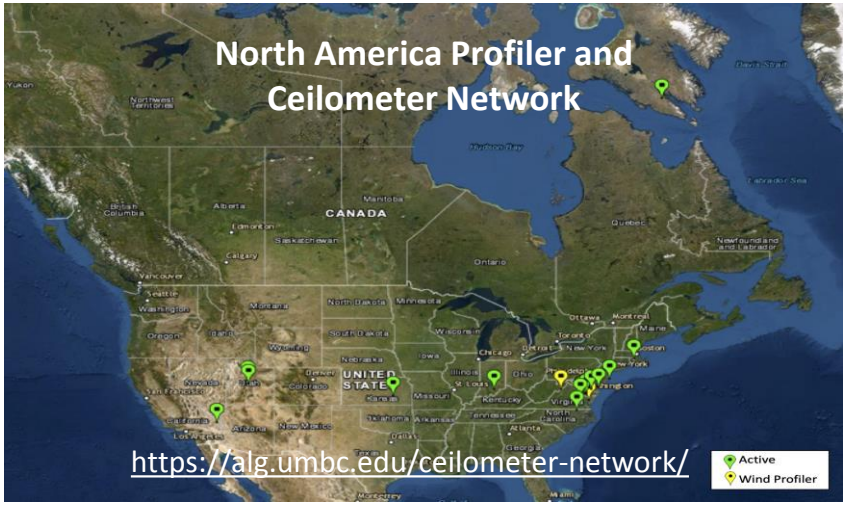

- Instrumentation:
  - Ceilometer, PANDORA, Auto GC
  - Ambient air database (met, $PM_{2.5}$, O_3, NO_2, NOx, speciated VOCs)
- Validation/verification satellite products and meteorological/air quality forecasts.

Ceilometer/Lidars

CCNY
UMBC
Howard Univ./Beltsville
Iqaluit, NU, CA
Providence, RI
Moose Hill, NH
Bristol, PA
Philadelphia, PA
Fair Hill, MD
Edgewood, MD
Essex, MD
Washington DC
Richmond, VA
Indianapolis, IN
Konza Praire, KS
Hawthorne, UT
Lindon, UT
Jerome Mack, NV

Radar Wind Profiler

Piney Run, MD
Howard Univ./Beltsville, MD
Horn Point Laboratory, MD

Coming Soon Online:

Blacksburg, VA
New Haven, CT
La Porte, TX
NASA JPL

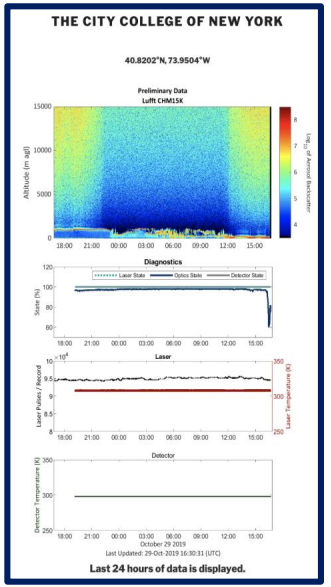

EPAMS Profiler and Ceilometer Network

Real-time Monitoring - Displays

Current Status

- Display of 15-60 minute data for all sites
  - Communication limitations = data frequecy data

- Real-time diagnostic parameters displayed for Lufft ceilometers
  - state of laser, detector, and optics; laser pulses; laser temperature; detector temperature

Vaisala Real-Time Display

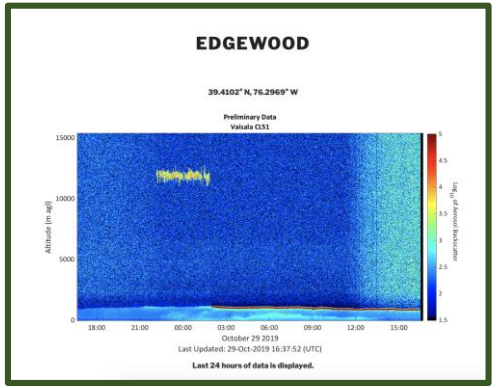

Lufft Real-Time Display

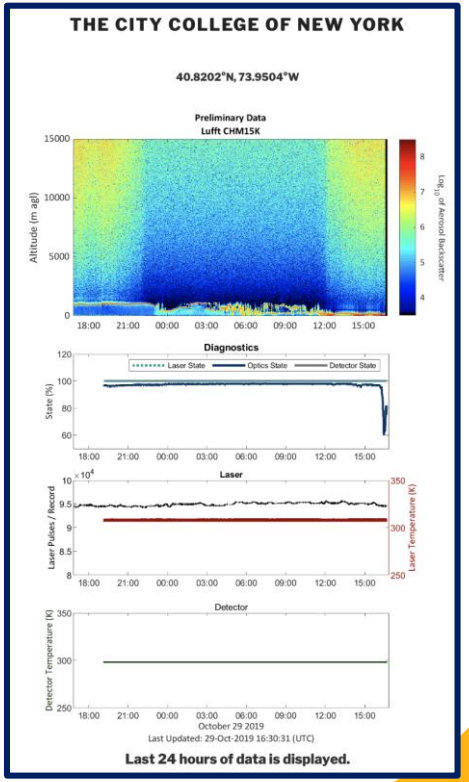

Next Steps

- Real-time retrievals for all sites (second server setup)
  - PBL and cloud heights
- Notification/Monitoring for diagnostic parameters
- Dynamic display

EPAMS Profiler and Ceilometer Network

Data Archive

Current Status

- Archiving all *'raw'* data from all sites
- Displaying archive images for all sites

Next Steps

- Download capabilities
  - Raw Data
  - Retrieval (MLH) Data
  - Data Export (NetCDf, h5, ASCII)
  - Quicklooks (jpeg, png)

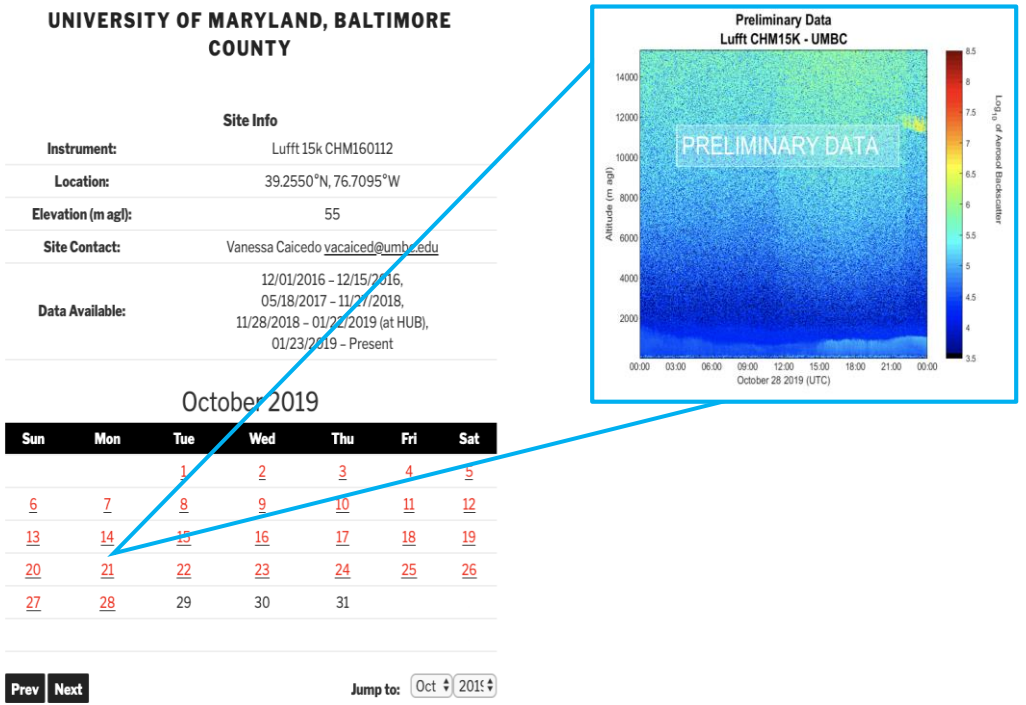

UNIVERSITY OF MARYLAND, BALTIMORE COUNTY

Site Info

Instrument:	Lufft 15k CHM160112
Location:	39.2550°N, 76.7095°W
Elevation (m agl):	55
Site Contact:	Vanessa Caicedo vacaiced@umbc.edu
Data Available:	12/01/2016 – 12/15/2016, 05/18/2017 – 11/21/2018, 11/28/2018 – 01/22/2019 (at HUB), 01/23/2019 – Present

October 2019

Sun	Mon	Tue	Wed	Thu	Fri	Sat
		1	2	3	4	5
6	7	8	9	10	11	12
13	14	15	16	17	18	19
20	21	22	23	24	25	26
27	28	29	30	31		

Prev Next Jump to: Oct 2019

Synergy Ground Networks and Satellite AQ

- **Real-time and Retrospective Analysis of Air Quality Events**
- **Correlation of Surface Mass Concentrations to Column Measurements**
  - Above/Below Mixing Layer Height
    - Aerosols: AOD-$PM_{2.5}$ Estimator (MODIS, VIIRS)
    - Ozone: TOLNET, PANDORA
- **Verification/Validation of Satellite Products and Models**
  - GOES 16/ABI: Smoke Plume Height Injection
  - TEMPO, MAIA

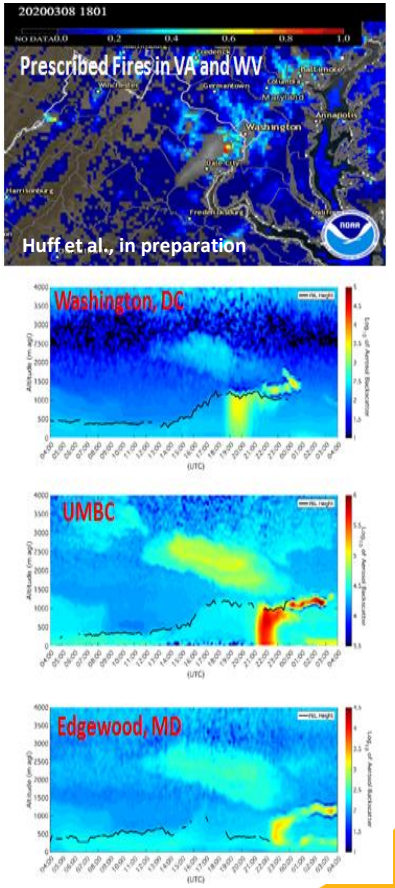

Exercise

- PBL for June 11, 2015 (16:20-16:40 UTC) from lidar data (Label region what you will consider the PBL and clouds).

- Visual determination of PBLH for March 8, 2020 event to be verified with two radiosonde parameters/variables: potential temperature (θ)and additional variable of your choice.
  - PBLH calculation

    Hefter Method: $\Delta\theta/\Delta z > 0.005$ K m^{-1}

    $\Delta\theta > 1.5$ K

- Rawinsondes and ceilometer/lidar data available in Ceilometer folder (Dropbox).

Exercise

- June 11, 2015:
  Time, Range Above Surface, 532 nm Total Attenuated Backscatter
- March 8, 2020:
  Time, Range, beta_raw

All files and Matlab reader (next slide) for netcdf file from Lufft ceilometer) in Dropbox:
PlotLufft.m

Contact Info (feel free to reach out):
Email: delgado@umbc.edu
Cell: 301-512-6638

```
%% Variables
%read backscatter profile, time, and altitude from file
InFile = '20200308_Catonsville-MD_CHM160112_000.nc';
Time = ncread(InFile,'time');
alt = ncread(InFile,'range');
Braw = ncread(InFile,'beta_raw');
Profile = double(Braw);
APA =Profile;
tt= log10(abs(Profile));

%reformat time
timevecUTC = datevec(Time/(3600*24) + datenum(1904, 1, 1, 0, 0, 0));
timewaveUTC = datetime(timevecUTC,'InputFormat','YYYY-MM-dd HH:mm:SS');
timenumUTC = datenum(timewaveUTC);

%% Plot backscatter
figure;
caxis=[3.5 8.5];
imagesc(timenumUTC,alt,tt,caxis);
datetick('x','HH:MM','keeplimits')%convets x-axis from serial num to time
h=colorbar;
ylabel(h,'Log_{10} of Aerosol
```

Acknowledgements

Maryland Department of the Environment
Environmental Protection Agency
NOAA Office of Education
NASA
Campbell Scientific
Lufft
Vaisala
Leosphere
NRG Systems

Backup Slides

Ad-hoc Ceilometer Evaluation Study

Retrieval Algorithm

1. Signal corrections (noise, artifacts, overlap, etc.)
2. Continuation parameters for layer attribution
3. Time-tracking height limitations to reduce misidentification of aerosol layers during transition times
4. Cloud identification independent of commercial cloud retrievals
5. Range of Haar wavelet transforms to calculate uncertainties in retrievals
6. Cloud classification in order to include convective cloud-topped boundary layers and cloud cover information
7. Define dilations and ranges based on uncertainties

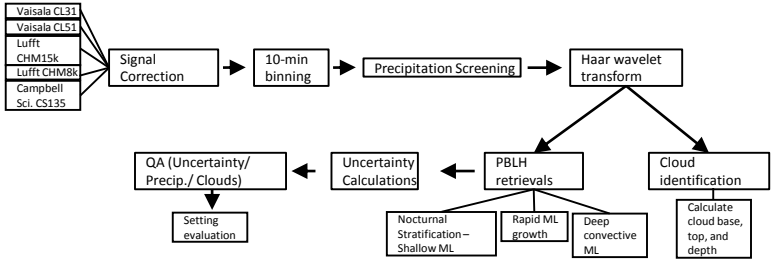

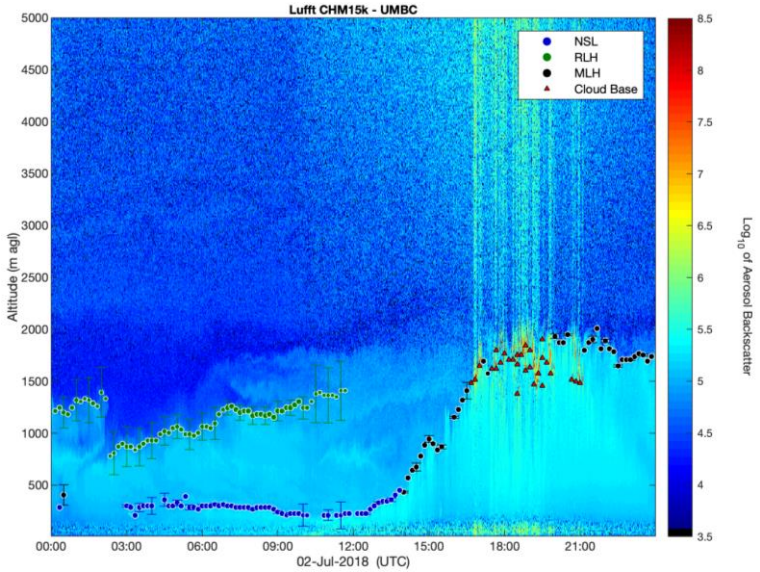

Caicedo et al. (2017, 2019)

Planetary Boundary Layer Height Algorithm

Covariance Wavelet Transform Algorithm

- **Automated** algorithm corrects for **instrument signal** quality and automatically **screens for precipitation and cloud layers**
- **Layer attribution** for the planetary boundary layer height with **continuation and time-tracking parameters**
- **Calculated uncertainties** in the **individual** planetary boundary layer height retrievals
  - Uncertainties >200m are automatically flagged as invalid

Table 3. Overall results of all comparison available for the study including linear regression correlation coefficient (r^2), slope of linear regression, offset of linear regression. Bias, and root-mean square error.

	CL51	CHM15k	CL31	CS135
r^2	0.96	0.86	0.90	0.90
Slope	0.90	0.96	0.96	0.97
Offset	116.75	75.16	27.39	134.52
Bias (m)	-12.66	-30.35	11.82	-108.31
RMSE (m)	94.33	208.31	156.83	168.88

Next Steps

- Automatic parameter selection
- Algorithm training

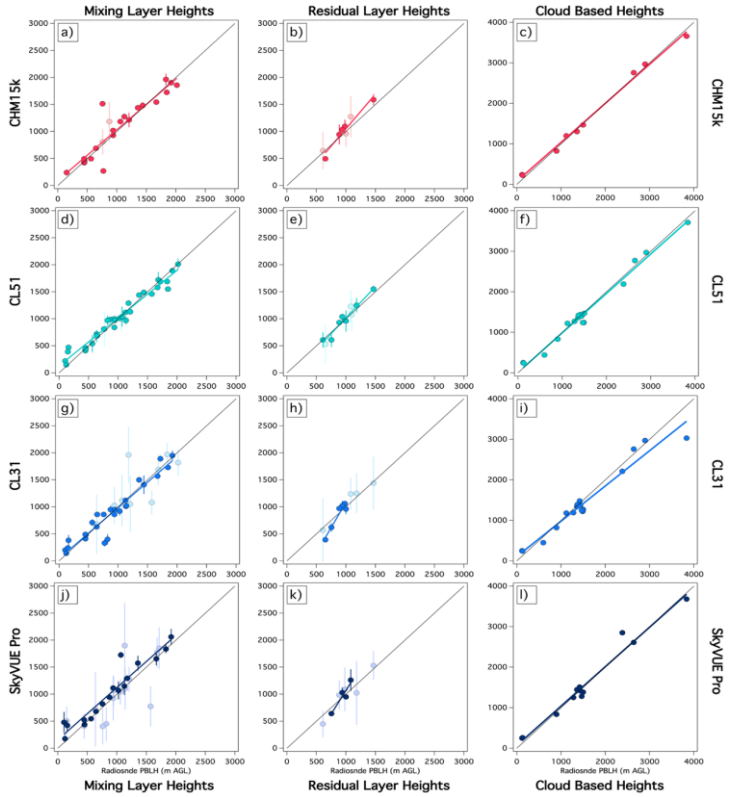

Searchlight → Modern Lidar

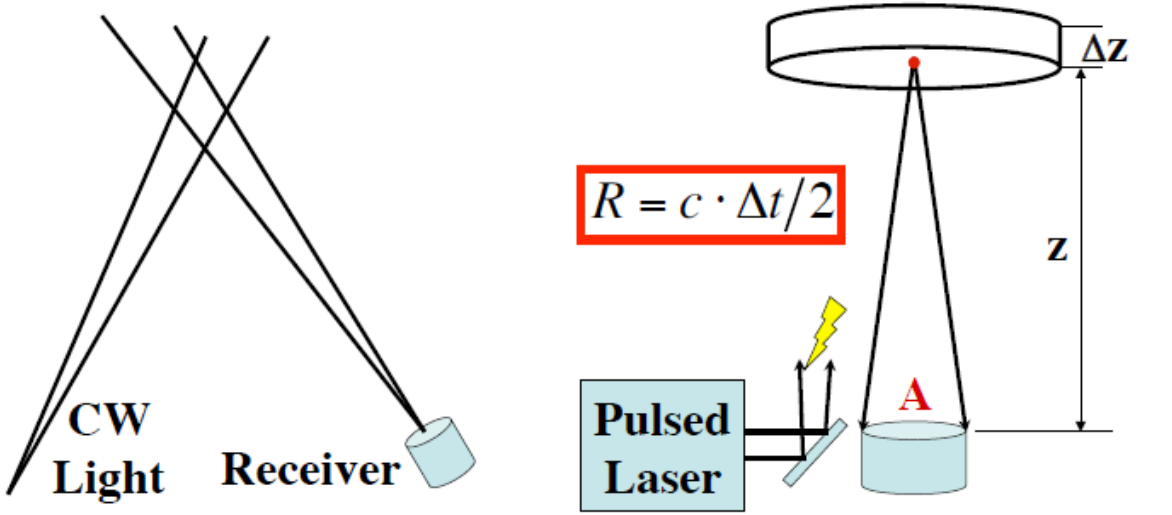

Bistatic Configuration Monostatic Configuration

CW searchlight → ns laser pulse

Altitude and Range Determination

- Searchlight lidar, cw laser lidar, and CCD-imaging lidar: determine altitude through the geometry calculation.

$$h = \frac{d \cdot \tan(\theta_T) \cdot \tan(\theta_R) + H_T \cdot \tan(\theta_R) + H_R \cdot \tan(\theta_T)}{\tan(\theta_T) + \tan(\theta_R)}$$

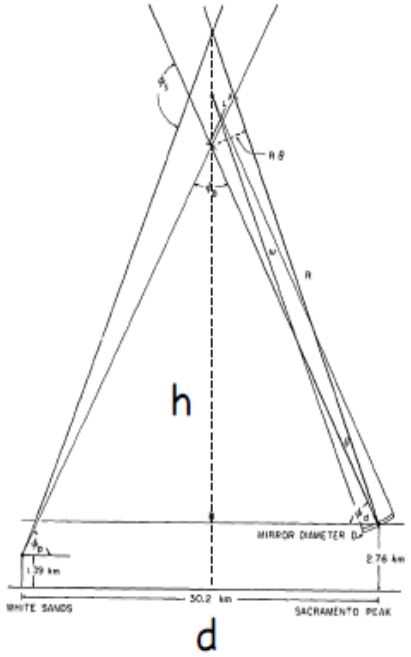

The Overlap Function O(R)

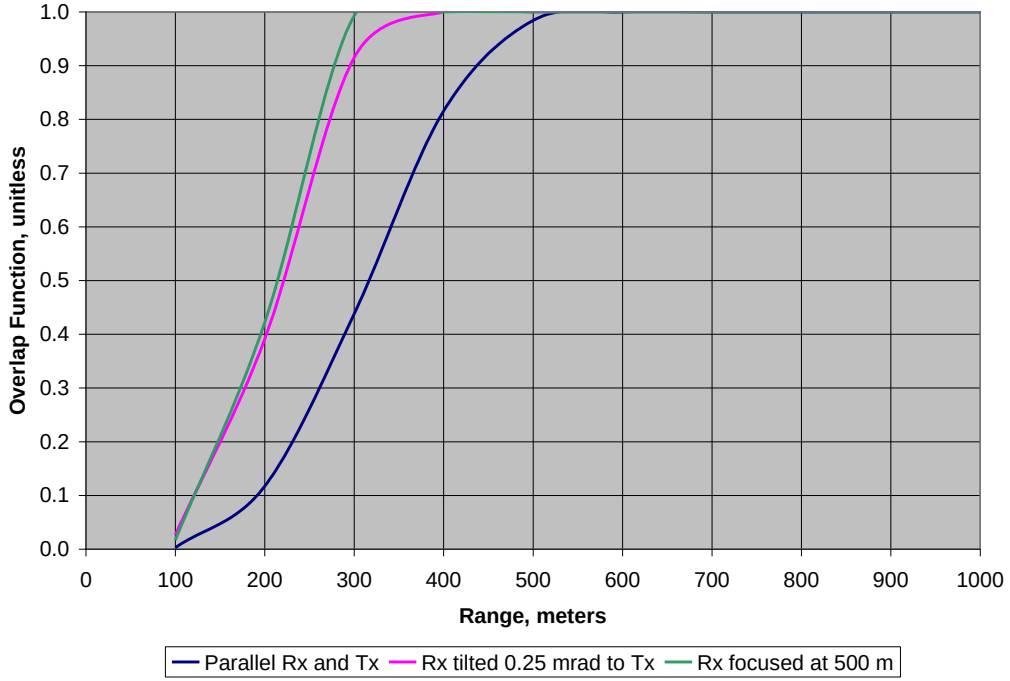

- The overlap function describes the range-dependent sensitivity of the receiver
- Demonstrates why lidars are so alignment sensitive

Adapted D. Roberts AMS 2007

Crossover

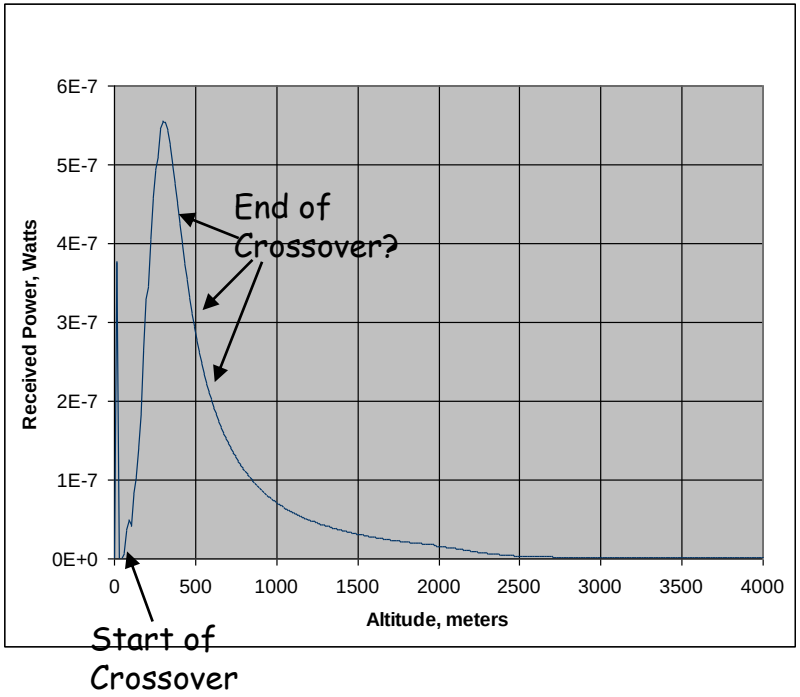

- The movement of the image into the field stop over a range of distances produces a phenomenon called “crossover”
- This phenomenon drastically affects the amount of light that reaches the receiver photodetector
- The start of crossover is obvious in the recorded signal
- The completion of crossover does not occur at the peak of the signal and does not have a corresponding feature that can be observed
- Only through careful design and system characterization can the completion of crossover be known

Adapted D. Roberts AMS 2007

General Equation Lidar in Terms of β and α

$$N_S(\lambda,R)=\left[\frac{P_L(\lambda_L)\Delta t}{hc/\lambda_L}\right]\left[\beta(\lambda,\lambda_L,\theta,R)\Delta R\right]\left(\frac{A}{R^2}\right)\cdot\exp\left[-\int_0^R\alpha(\lambda_L,r')dr'\right]\exp\left[-\int_0^R\alpha(\lambda,r')dr'\right]\left[\eta(\lambda,\lambda_L)G(R)\right]+N_B$$

β is the volume scatter coefficient

α is the extinction coefficient

Volume scatter coefficient $$\beta(\lambda,\lambda_L,R)=\sum_i\left[\frac{d\sigma_i(\lambda_L)}{d\Omega}n_i(R)p_i(\lambda)\right]$$

Transmission $$T(\lambda_L,R)T(\lambda,R)=\exp\left[-\left(\int_0^R\alpha(\lambda_L,r)dr+\int_0^R\alpha(\lambda,r)dr\right)\right]$$

Light Propagation through the Atmosphere

- When light propagates through the atmosphere or medium, it experiences attenuation (extinction) caused by absorption and scattering of molecules and aerosol particles.

Transmission + Extinction = 1

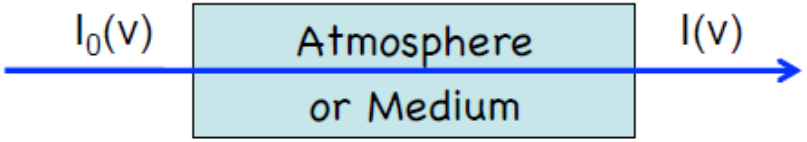

$$Transmission = \frac{I(\nu)}{I_0(\nu)} \quad (5.1), \qquad Extinction = \frac{I_0(\nu) - I(\nu)}{I_0(\nu)} \quad (5.2)$$

- The energy loss of a laser beam propagating through the atmosphere is due to molecular absorption, molecular scattering, aerosol scattering and aerosol absorption.

Molecular Absorption

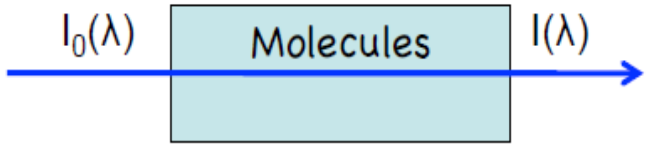

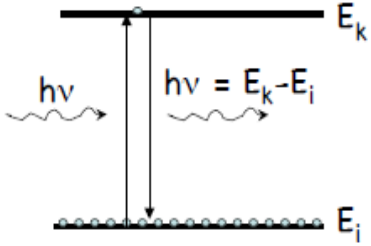

- The intensity change dI of a light propagating through an absorbing sample is determined by the absorption coefficient $\alpha_{mol,abs}$ in the following manner:

$$dI(\lambda) = -I(\lambda)\alpha(\lambda)dz = -I\sigma_{ik}(\lambda)(N_i - N_k)dz \qquad (5.3)$$

$\alpha(\lambda) = \sigma(\lambda)(N_i - N_k)$ is absorption coefficient caused by transition $E_i \rightarrow E_k$
Here, σ_{ik} is the absorption cross section, N_i and N_k are the populations on the energy levels of E_i and E_k, respectively.

- If $\Delta N = N_i - N_k$ is independent of the light intensity I, the absorbed intensity dI is proportional to the incident intensity I (linear absorption). Solving the above equation, we obtain

$$I(\lambda,z) = I_0 \exp\left[-\int_0^z \sigma_{ik}(\lambda)(N_i - N_k)dz\right] \qquad (5.4)$$

$$\rightarrow \quad I(\lambda,z) = I_0 e^{-\sigma(\lambda)(N_i - N_k)L} = I_0 e^{-\alpha(\lambda)L}$$

-- Lambert-Beer's Law (5.5)